Received: 29 November 2022 | Revised: 23 December 2022 | Accepted: 1 January 2023

DOI: 10.1002/smm2.1185

REVIEW

SmartMat Open Access WILEY

Recent progress in electrolyte design for advanced lithium metal batteries

Mingnan Li | **Caoyu Wang** | **Kenneth Davey** | **Jingxi Li** | **Guanjie Li** | **Shilin Zhang** | **Jianfeng Mao** | **Zaiping Guo**

School of Chemical Engineering & Advanced Materials, The University of Adelaide, Adelaide, Australia

Correspondence
Jianfeng Mao and Zaiping Guo, School of Chemical Engineering & Advanced Materials, The University of Adelaide, Adelaide, SA 5000, Australia.
Email: jianfeng.mao@adelaide.edu.au and zaiping.guo@adelaide.edu.au

Funding information
Australian Research Council, Grant/Award Numbers: DP210101486, FL210100050, LP160101629

Abstract

Lithium metal batteries (LMBs) have attracted considerable interest for use in electric vehicles and as next-generation energy storage devices because of their high energy density. However, a significant practical drawback with LMBs is the instability of the Li metal/electrolyte interface, with concurrent parasitic reactions and dendrite growth, that leads to low Coulombic efficiency and poor cycle life. Owing to the significant role of electrolytes in batteries, rationally designed electrolytes can improve the electrochemical performance of LMBs and possibly achieve fast charge and a wide range of working temperatures to meet various requirements of the market in the future. Although there are some review papers about electrolytes for LMBs, the focus has been on a single parameter or single performance separately and, therefore, not sufficient for the design of electrolytes for advanced LMBs for a wide range of working environments. This review presents a systematic summary of recent progress made in terms of electrolytes, covering the fundamental understanding of the mechanism, scientific challenges, and strategies to address drawbacks of electrolytes for high-performance LMBs. The advantages and disadvantages of various electrolyte strategies are also analyzed, yielding suggestions for optimum properties of electrolytes for advanced LMBs applications. Finally, the most promising research directions for electrolytes are discussed briefly.

KEYWORDS

anion-derived SEI, fast charge, liquid electrolyte design, lithium metal batteries, safe electrolytes, wide working temperature

1 | INTRODUCTION

In traditional lithium ion batteries (LIBs) with graphite as the anode and lithium layered oxide/lithium iron phosphate as the cathode, Li^+ insert into graphite and de-insert from graphite to achieve energy storage.[1–4] The use of graphite with high capacity (375 mAh/g), low potential, and less volume change during the charge/discharge process confers LIBs high energy density and long lifespan. However, with the rapid development of

FIGURE 1 Illustration of the requirements for future advanced lithium metal batteries.

electric vehicles (EVs), current LIBs cannot meet the increasing demand.[5–10] In addition to high energy density, high-performance energy storage together with long lifespan, fast charging capability,[11] wide range of working temperatures, good safety, and low cost are needed for a range working conditions, Figure 1.[12]

The lifespan of current LIBs is ca. 10–15 years in small electronics and ca. 8–10 years in EVs.[13] Harsh working conditions accelerate decay in battery performance, leading to frequent battery replacements and high costs. Long lifespan batteries decrease maintenance costs. It is desired, therefore, that the next-generation energy storage devices have lifespans equivalent to or greater than that for LIBs. Fast charging capability is a core performance parameter for rechargeable batteries, especially for EVs.[14,15] Conventional EVs take some hours to be fully charged, certainly longer than that for filling internal combustion engine vehicles with fuel. For practical applications, it is important, therefore, to have EV batteries that can be fully charged in <0.5 h or even a few min. Energy storage devices are also important in the oil industry and deep-sea and aerospace exploration, therefore, there is a required for batteries with wide range of working temperatures.[16,17] However, current LIBs lose significant capacity and power when the temperature is <0°C because of high ion-transport resistance and a low reaction rate.[18] Accelerated side reactions at elevated temperatures also lead to cell failure, resulting in poor cycling performance and decreased safety.[19] These drawbacks will need to be addressed to promote advancement of next-generation energy storage devices.

Li metal is an almost "ideal" anode that has therefore received considerable research attention[20] because of a high capacity of 3860 mAh/g and the lowest chemical species redox potential of 3.04 V versus a standard hydrogen electrode.[21] Lithium metal batteries (LMBs) with high energy density have been promising for next-generation energy storage; however, development has been limited due to the instability of the Li metal/electrolyte interface, with concurrent parasitic reactions and dendrite growth[22–24] during battery cycling, resulting in poor Coulombic efficiency (CE) and reduced cycle life. Large dendrites can pierce the separator, leading to short circuit, thermal runaway, and even explosion.[25] Poor electrochemical performance and reduced safety, therefore, limit the application of Li anodes.

The electrolyte is an essential component in batteries; it acts as the media for ion transport between positive and negative electrodes. Highly reactive Li metal reacts with most liquid electrolytes, consuming Li^+ ions. However, Li metal was found to be stable in a number of nonaqueous solvents because of the formation of a passivation solid electrolyte interphase (SEI) film on the Li surface.[26–30] The electronically insulating and ionic conductive SEI prevents direct contact between the electrolyte and Li, resulting in stable Li stripping/plating. The microstructure, morphology, and chemical composition of SEI are closely related to the electrolyte. Reports confirm that the rational design of electrolytes facilitates the formation of SEI with strong passivation ability to enable stable Li plating/stripping.[31–35] By tuning the electrolyte via selection and optimization of solvents, Li salts, and electrolyte additives, electrochemical performance, including the wide range of working temperatures[36,37] and fast charging capability,[38,39] is significantly improved. Therefore, high-performance LMBs can be developed via the targeted design of electrolytes.

In this review, we focus on methods for the design of electrolytes for advanced LMBs.

2 | ACHIEVING LONG LIFESPAN LMBs

LMBs show a shorter lifespan than LIBs. In LIBs, the conventional electrolyte component, ethylene carbonate (EC), decomposes at the graphite anode and forms stable SEI, resulting in a high CE. The Li anode also reacts with nonaqueous electrolytes to form SEI; however, large volume change during charge/discharge causes SEI fracture. Dendrite formation during battery cycling also results in the destruction of the SEI layer on the Li metal anode. Dendrites form because of sluggish Li^+ ion diffusion that leads to uneven Li electrodeposition.[40]

Higher electric field at the tips tends to attract additional Li^+, resulting in further growth of protrusions, finally evolving into dendrites. The volume change and dendrites cause a destruction of the original SEI and more "native" Li is exposed to the electrolyte. As a result, the electrolyte reacts with Li, resulting in continuous consumption of the electrolyte, a "thickened" SEI layer, and large internal resistance, and thus decreases CE. This continues until the battery fails operationally. Therefore, formation of a stable SEI is important to ensure stable Li stripping/plating and long lifespan in LMBs.

2.1 | Formation of a robust SEI

SEI is usually derived from Li^+, solvent, and anion decomposition. Anions include fewer C atoms and more S, F, and P, which likely form inorganic compounds with high interfacial energy to passivate the Li anode and boost performance.[39,41,42] Therefore, targeted methods have been reported for the formation of anion-derived SEI.

2.1.1 | High-concentration electrolyte (HCEs) and localized high-concentration electrolytes (LHCEs)

HCEs have been shown to produce anion-derived SEI. The common concentration of electrolyte is 1 mol/L, given the impact of ion conductivity, cost, and viscosity. In these electrolytes, solvent molecules occupy the first coordination shell of Li^+, leading to a full solvation structure or a solvent-separated ion pair (SSIP) as shown in Figure 2A. However, the full solvation structure will decrease the lowest unoccupied molecular orbital (LUMO) of solvents, leading to preferential solvent decomposition on Li metal anodes.[44] Solvent-derived SEI with more organic compounds has poor passivation ability.[39] In HCEs, interaction of Li^+ with multiple anions and fewer solvent molecules leads to the formation of contact ion pairs (CIPs) and aggregates (AGGs). With less SSIP and free solvent molecules, the anion with lower LUMO is preferentially reduced to form an anion-derived SEI with low interfacial resistance, Figure 2B.[41,45] Use of HCEs is a very useful method to introduce anion-derived SEI, and a number of HCEs have been investigated, including lithium bis(fluorosulfonyl) imide (LiFSI)/dimethoxyethane (DME),[46] LiFSI/Trimethyl phosphate (TMP),[47] LiFSI/dimethyl carbonate (DMC),[48] LiFSI/sulfolane (SL),[49] lithium bis(trifluoromethanesulfonyl)imide (LiTFSI) + lithium difluoro(oxalate)borate (LiDFOB)/DME,[50] and LiDFOB + lithium tetrafluoroborate ($LiBF_4$)/fluoroethylene carbonate (FEC): diethyl carbonate (DEC),[51] LiFSI/tetrahydrofuran (THF)[52], and LiFSI/FEC electrolytes.[53] HCEs have additional advantages in batteries as they promote anion-derived SEI formation including widening of the electrochemical window and operation temperatures of the cell, preventing corrosion of the

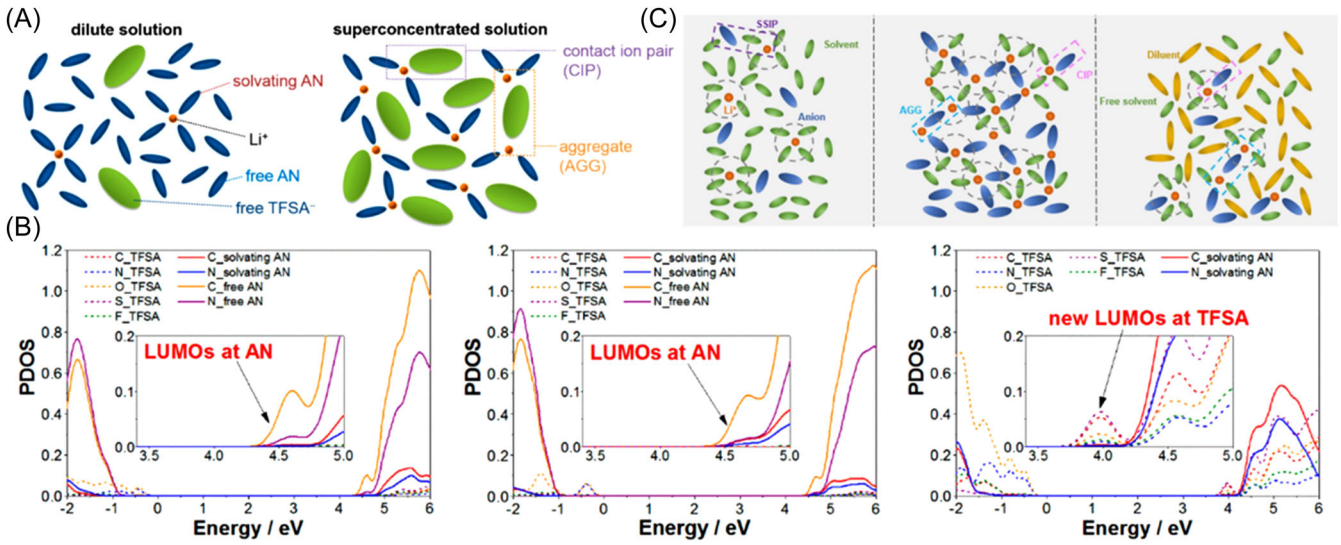

FIGURE 2 (A) Environment for Li^+ in 1 mol/L and HCEs of an ACN-based electrolyte. Reproduced with permission.[39] Copyright 2014, American Chemical Society. (B) Projected density of states obtained from quantum mechanical DFT-MD simulations on SSIP (left), CIPs (middle) in 1 mol/L, and HCEs (right) of an ACN-based electrolyte. Reproduced with permission.[39] Copyright 2014, American Chemical Society. (C) Schematic for solution structure: conventional dilute (left), concentrated (middle), and diluted concentrated (right) electrolyte. Reproduced with permission.[43] Copyright 2022, American Chemical Society. ACN, acetonitrile; CIP, contact ion pair; HCE, high-concentration electrolyte; LUMO, lowest unoccupied molecular orbital; MD, molecular dynamics; SSIP, solvent-separated ion pair.

current collector. To overcome the high viscosity and the low ion conductivity of HCEs, localized LHCEs were proposed, Figure 2C.[43,54–56] LHCEs make use of an inert solvent that is unable to solvate with Li^+, such as hydrofluoroethers, including 1,1,2,2-tetrafluoroethyl-2,2,3,3-tetrafluoropropyl ether (TTE),[57,58] tris(2,2,2-trifluoroethyl) orthoformate (TFEO)[59], and (2,2,2-trifluoroethyl) ether (BTFE)[60] to dilute HCEs. In this way, the viscosity of the electrolyte is reduced, giving good wetting to the separator and electrode. The high cost and high viscosity of HCEs limit their large-scale application; LHCEs, which can decrease viscosity and improve electrochemical performance, are a better choice for application.

2.1.2 | Fluorinate–ether solvent

In addition to HCEs and LHCEs, fluorinate–ether electrolytes can be used to modulate the Li^+ solvation environment and generate inorganic-enriched SEI. In 2,2-dimethoxy-4-(trifluoromethyl)-1,3-dioxolane (DTDL) fluorinate–ether electrolytes, Raman spectra show more AGGs in the DTDL electrolyte compared with the DME electrolyte, confirming more anion coordination with Li^+ in the DTDL electrolyte, Figure 3A–C.[61] As a result, a stable CE of 99.2% following 500 cycles was shown using DTDL electrolyte with a high-voltage cathode in LMBs. For fluorinated 1,4-dimethoxylbutane (FDMB), 1,4-dimethoxylbutane (DMB), and DME electrolytes, molecular dynamics (MD) simulation showed an average ratio of FSI^-/solvent molecules of 2.31:1 for DME and 2.29:1 for DMB in the Li^+ solvation shell.[62] However, the FSI^-/solvent ratio in the Li^+ solvation sheath is highly significantly increased to 3.29:1 in 1 mol/L LiFSI/FDMB, confirming that FDMB performs poorly in dissociating ion pairs and preferentially forms anion-derived SEI. 1 mol/L LiFSI/FDMB, therefore, showed a high CE of 99.52% in Li||Cu half-cells.

The degree of fluorination impacts the solvation structure. The partially fluorinated, asymmetric $-CHF_2$ group showed more electron negativity to enable strong intermolecular interactions in the solvent and better Li^+ solvation than an all-fluorinated, symmetric counterpart, $-CF_3$.[32] The F5DEE electrolyte with partial fluorination concurrently dissociates Li salt and has high ionic conductivity, fast and stable interfacial transport, high Li metal efficiency of up to 99.9% within Li||Cu half-cells, fast activation with CE > 99.3% from the second cycle in Li||Cu half-cells, and high voltage stability. Fluorination is a practically useful method to decrease the dielectric constant (ε), which significantly impacts the dissociation of Li salt.[63] With lower ε, the salt fails to dissociate

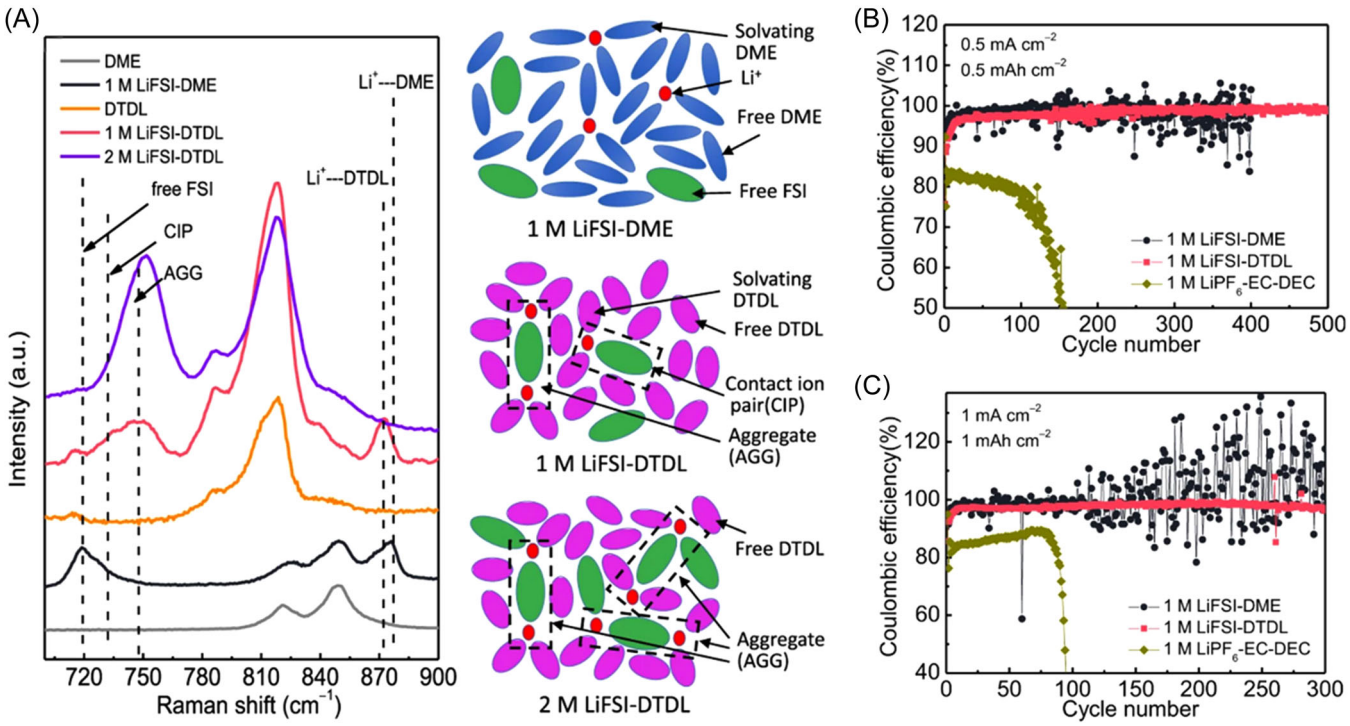

FIGURE 3 (A) Raman spectra of solvents and electrolytes and schematic diagrams of Li^+ coordination structures in different electrolytes. Cycling stability of Li||Cu half-cells using different electrolytes at (B) 0.5 mA/cm^2 and (C) 1 mA/cm^2. Reproduced with permission.[61] Copyright 2022, Springer Nature.

completely, forming less SSIP and more CIPs and AGGs. Unlike hydrofluoroethers, which have limited salt solubility, the introduction of –F in the ether electrolyte balances solvation ability and oxidation stability and optimizes the solvation shell to form anion-derived SEI. However, current research on fluorinate–ethers is ongoing and most fluorinate–ethers are not commercially available. The complex chemical synthesis is not cost-effective and is therefore a drawback for large-scale application. Ionic conductivity is determined by the number of SSIP and free anions. Fluorination of solvents can weaken the solvated interaction between Li^+ and solvents, leading to less SSIP and low ion conductivity. Therefore, an optimal balance between the solvation structure and ion conductivity is needed for improved battery performance.

2.1.3 | Additives for SEI

The introduction of other anions mediates the solvation structure, which leads to preferred anion decomposition. For lithium nitrite ($LiNO_3$) additives, Raman findings show that NO_3^- enters in the solvation shell of Li^+, changing the reduction behaviors of electrolytes, Figure 4A.[64,66–68] With the exception of NO_3^-, other electrolytes with different anions, including LiTFSI/LiFSI (additives),[69] LiFSI/$LiClO_4$,[70] and LiTFSI/LiDFOB,[38,71] influence the Li^+ solvation environment to achieve better electrochemical performance. The electrophilic anion receptor that assists Li salts to dissociate influences the Li^+ solvation environment. For example, tris(pentafluorophenyl)borane (TPFPB) with an electron-deficient boron atom, can directly interact with FSI^-.[72] The LUMO energy level for FSI^- is reduced following interaction with TPFPB through B–F and B–O interactions, showing that the reduction stability of FSI^- in TPFPB-LHCE is reduced. Therefore, decomposition of FSI^- is promoted. A similar phenomenon occurs in the $LiNO_3$-based electrolyte with TPFPB, as shown in Figure 4B,C.[65] A lower LUMO energy is evident in TPFPB–NO_3^- of 2.05 eV compared with that in Li^+–NO_3^- of 1.90 eV, confirming the reduced reductive stability of TPFPB–NO_3^- compared with Li^+–NO_3^- for favorable reduction. These additives dissolve in the electrolyte to modulate the Li^+ ion solvation shell; however, some suspension electrolytes using nanoparticles with limited solubility in the electrolyte can influence the solvation environment. In a suspension electrolyte (1 mol/L $LiPF_6$ in EC/DEC/10 vol% FEC with Li_2O nanoparticles), Li_2O modify Li^+ solvated environment through interfacial interactions between the Li_2O surface and liquid electrolyte.[73] The suspension carbonate electrolyte induces inorganic-rich SEI, resulting in an improvement in CE to ~99.7%. Although nanoparticles including Li_2O,[73] LiF,[74] metal–organic framework,[75] and SiO_2[76] are insoluble in common electrolytes, the presence of a solid in the electrolyte influences the local solvation environment, usually near the particle surface. These insoluble particles can be used as multifunctional additives, specifically for oxidation stability and as fire retardants.[74] Particle size has a significant impact on electrolyte stability. Larger microparticles can "fail" to disperse sufficiently and generate precipitates in suspension; the resulting inhomogeneous electrolyte leads to unstable electrochemical performance. The addition of particles increases viscosity, and absorption between Li^+ and particles decreases ion diffusion and de-solvation.

These additives improve performance by modifying the solvation environment; however, another type of additive "sacrifices" itself to form a stable SEI in the Li anode. For example, FEC usually shows the lowest LUMO in common electrolytes because of the strong electro-withdrawing property of F-containing functional groups. FEC will preferentially be reduced to form stable SEI on the Li anode.[77–80] Similar to FEC, lithium difluorophosphate ($LiPO_2F_2$) has lower LUMO compared with EC and DMC, which shows that $LiPO_2F_2$ is reduced before the solvent.[81,82] The introduction of $LiPO_2F_2$ can generate LiF-enriched SEI to boost electrochemical performance. Vinylene carbonate (VC) is a widely recognized and used functional electrolyte additive in LIBs and LMBs. The polymeric-type species decomposed from VC generates surface films on the Li anode to suppress dendrites.[83] A number of boron-containing salts generate borate to yield stable SEI including LiDFOB[84] and lithium bis(oxalato)borate (LiBOB).[85–89] Compared with nanoparticle additives and anion receptor additives, "sacrificing" additives are those most reported. However, because these are consumed during cycling, the protection mechanism can fail following long cycling. A comparative summary of CE in selected electrolytes is presented in Table 1.

CE is an important parameter for the electrochemical performance of LMBs. However, at laboratory scale, CE is not an accurate predictor of the lifespan of batteries because Li is usually in excess in LMBs. Side reactions consume Li^+ and reduce CE; however, excess Li can be used to finish charge/discharge and boost CE. This is one contributor to LMBs at CE values close to 100% short unexpectedly and without warning signs. To accurately determine CE, it is necessary to follow the strict criterion of limited Li (less N/P ratio) and a lean electrolyte.

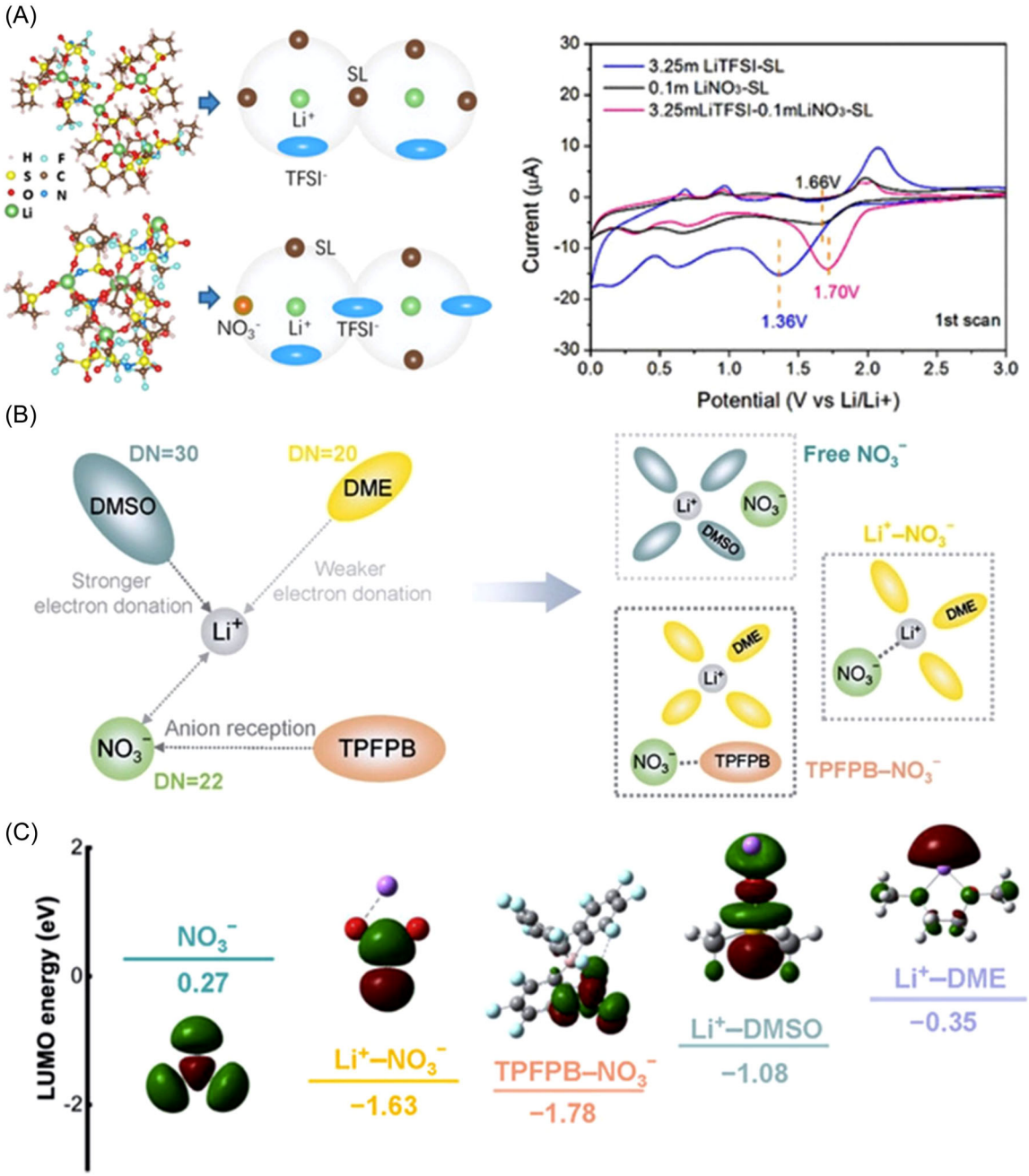

FIGURE 4 (A) Structure from MD simulation and schematic for 3.25 mol/L LiTFSI⁻SL (above) and 3.25 mol/L LiTFSI⁻0.1 mol/L $LiNO_3$–SL (below) electrolyte. Initial cyclic voltammetry curve for electrolytes between 0 and 3 V (vs. Li^+/Li). Reproduced with permission.[64] Copyright 2020, Wiley-VCH. (B) Coordination structure of NO_3^- in a nonaqueous electrolyte. Reproduced with permission.[65] Copyright 2021, Wiley-VCH. (C) LUMO energy and corresponding optimized geometrical structure for different electrolytes. Reproduced with permission.[65] Copyright 2021, Wiley-VCH. DME, dimethoxyethane; DMSO, dimethyl sulfoxide; LUMO, lowest unoccupied molecular orbital; MD, molecular dynamics; SL, sulfolane.

Parasitic reactions between the electrolyte and the cathode can also have a highly significant impact on lifespan. However, different cathodes show differing charge/discharge mechanisms, accompanied by different side reactions, for example, nickel-rich layered transition-metal oxide cathode materials including Li-$Ni_xCo_yMn_zO_2$ (NCM*xyz*) and sulfur cathode.

2.2 | Preventing Al corrosion in high-voltage cathodes

Usually, cathodes are obtained via casting of active material onto a current collector. Al with high electro-conductivity and low cost is widely used as a cathode current collector. Although Al has a redox potential of

TABLE 1 Coulombic efficiency (CE) of Li||Cu in selected nonaqueous electrolytes.

Electrolyte	Average CE (%)	Current density (mA/cm^2)	Area capacity (mAh/cm^2)	Cycle number
1.2 mol/L LiFSI F5DEE[32]	99.74	0.5	1	500
1 mol/L LiFSI DTDL[61]	99.20	0.5	0.5	250
4 mol/L LiFSI DEE[31]	99.25	0.5	1	150
1 mol/L LiFSI FDMB[62]	99.52	0.5	1	50
3.25 mol/L LiTFSI SL + 0.1 mol/L $LiNO_3$[64]	98.5	0.5	1	100
1 mol/L $LiPF_6$ EC/DEC/EMC/FEC (28:28:28:16, volume ratio) + 10 wt% LiF[74]	98	0.5	1	500
1 mol/L $LiPF_6$ FEC/DME (3:7, volume ratio) + 0.65 mol/L $LiNO_3$[67]	98	0.5	1	450
$LiFSI^-$SL-BTFE (1:3:3, molar ratio)[90]	98.8	0.5	1	150
7 mol/L LiFSI FEC[53]	98.8	0.25	0.5	400
1.8 mol/L LiFSI DMC/BTFE (1:1.5, molar ratio)[54]	99.5	0.5	1	200
1 mol/L $LiPF_6$ EC/DMC (1:1, volume ratio) + 5 vol% FEC + 5 vol% of 3.4 mol/L $LiNO_3$ in G4 + 0.01×10^{-3} mol/L I_2[91]	98.27	0.5	1	200
1 mol/L $LiPF_6$–FEC/FEMC/TTE (2:6:2 by weight)[58]	99.2	0.2	1	500
0.3 mol/L LiTFSI + 0.3 mol/L THF FM/CO_2 (19:1, weight ratio)[92]	99.4	0.5	0.5	200
5 mol/L LiTFSI EMImTFSI + 0.16 mol/L NaTFSI[93]	99	0.5	0.5	400
1 mol/L $LiPF_6$ EC/DEC/FEC (4:4:2) + 40% (volume ratio) 3 mol/L $LiNO_3$ TMP[68]	99.49	0.25	1	100

1.364 V (vs. Li^+/Li), the Al_2O_3 derived via air can generate a dense, protective layer, leading to stable cycling in LMBs.[94] However, Al dissolution will occur on using an NCM cathode, which has high charge/discharge potential.[95,96] In commercial LIBs, trace amounts of water hydrolyze $LiPF_6$ to produce HF, which subsequently reacts with Al to form a stable AlF_3 film on the surface and passivate Al.[94] However, with LiTFSI, Al^{3+} will interact with $TFSI^-$ to form highly soluble $Al(TFSI)_3$ in the electrolyte, leading to worse current collector corrosion.[97] Al corrosion destroys the integrity of the electrode and influences electron transfer between the current collector and active material to decrease the electron conductivity of the electrode and lead to fast capacity decay. Because the choice of Li salt has a significant impact on Al corrosion, new Li salts, including LiBOB[98] and LiDFOB,[99,100] are reportedly used to suppress Al corrosion. However, these anticorrosion salts have limited solubility and poor conductivity in carbonate and ether electrolytes, limiting their application. Use of a noncorrosive salt, lithium (difluoromethanesulfonyl)(trifluoromethanesulfonyl)imide (Li[$N(SO_2CF_2H)(SO_2CF_3)$], LiDFTFSI), as the main salt in electrolytes has been reported.[101] The LiDFTFSI-based carbonated electrolyte exhibited 3.7 mS/cm ionic conductivity and high anodic stability of 5.6 V versus Li^+/Li. In contrast to a typical LiTFSI-based electrolyte, the LiDFTFSI-based electrolyte has good compatibility with the Al current collector at high potential of ca. 4.2 V versus Li^+/Li because unstable Al $(DFTFSI)_3$ decomposes to form AlF_3 with strong passivation ability, protecting the Al current collector from further anodic dissolution. Therefore, there is better cycling stability in coin cells using a LiDFTFSI-based electrolyte. With current LMBs and LIBs, there are a significant number of electrolytes, but the choice of Li salts for LMB application is limited. Therefore, exploration of new Li salts is needed. However, it is important to optimize cost, safety, and electrochemical performance.

HCEs are useful for Al protection. LiFSI/DMC-based HCEs suppress Al corrosion, even at >5 V (vs. Li^+/Li), while continuous Al dissolution occurs in the dilute LiFSI/DMC electrolyte at 4.3 V (vs. Li^+/Li) that leads to "unlimited" overcharging, Figure 5.[48] In LiFSI/DMC-based LHCEs, there is reduced pitting of the Al current collector and CE is boosted.[54]

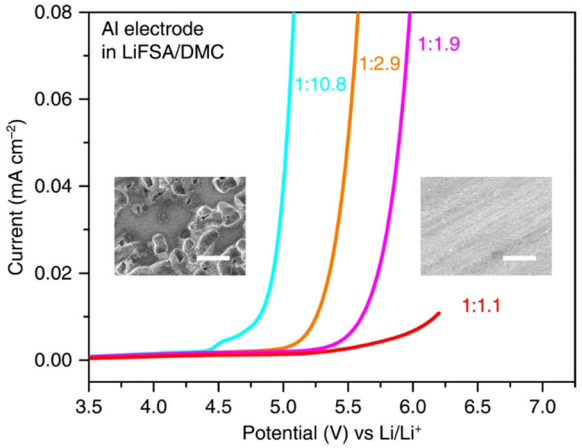

FIGURE 5 Linear sweep voltammogram of an Al electrode at various concentrations of LiFSI (or LiFSA)/DMC electrolytes in a three-electrode cell with 1.0 mV/s. The insets show scanning electron microscopy images of the Al surface cycled in dilute 1:10.8 (left) and superconcentrated 1:1.1 (right) electrolytes. The white scale bar represents 20 μm. Reproduced with permission.[48] Copyright 2016, Springer Nature. DMC, dimethyl carbonat; LiFSA (or LiFSI), lithium bis(fluorosulfonyl) imide.

2.3 | Constructing stable cathode–electrolyte interface (CEI) in high-voltage cathodes

The use of high-voltage cathodes poses practical difficulties in terms of structural instability, phase transition, transition-metal dissolution, and release of oxygen gas, which lead to continuous decomposition of the electrolyte at the interface.[102–104] Similar to SEI in the anode, CEIs form on cathodes and impact the performance of secondary batteries. Currently, an optimized CEI is obtained using additives such as LiBOB,[105] LiDFOB,[106] lithium difluorobis(oxalato) phosphate (LiDFBOP),[107] and $LiPO_2F_2$[108] that prefenertially oxidize at the cathode surface to form robust and stable CEI composed of inorganic-rich components. The highest occupied molecular orbital (HOMO) of VC is higher than that for EC, respectively, for VC and EC: −10.26 and −12.76 eV. VC is more readily oxidized at the positive electrode surface than EC, preferentially forming a passive layer on the electrode.[109,110] FEC is reported to be a useful additive to boost the formation of CEI because the decomposition of FEC yields an F-rich passivated layer.[111] These additives improve SEI and promote the formation of CEI because additives containing F, B, and P elements will eventually decompose F-, B-, and P-containing compounds to isolate and prevent direct contact between the electrolyte and the electrode. However, from another point of view, additives facilitate the formation of CEI and SEI via different mechanisms. For FEC, a lower LUMO promotes preferential reduction to form LiF-enriched SEI; however, FEC as a nonsacrificial additive boosts CEI stability via modification of the solvation structure.[112] It is also possible that the compounds formed in the compact and thin CEI layers on the cathode diffuse from the anode side.[113]

2.4 | Preventing shuttle effect in Li–S cells

Sulfur cathodes with high capacity and high energy density have been reported as next-generation cathodes. Because of nucleophilic side reactions between carbonate electrolytes and lithium polysulfide (LiPS) species, ether electrolytes are commonly used in Li–S cells.[114,115] However, LiPS has high solubility in ether electrolytes, leading to fast capacity fade and decreased CE. In recent decades, researchers have focused on cathode modification to prevent the shuttle effect caused by high LiPS solubility.[116,117] However, rational electrolyte design can also suppress the shuttle effect to induce higher capacity retention.

In HCEs and LHCEs, there is limited LiPS solubility, which significantly suppresses the shuttle effect to improve cycling stability. The 7 mol/L LiTFSI in dioxolane (DOL)/DME electrolyte prompts anion-derived SEI against formation of Li dendrites that boosts Li–S cells to exhibit excellent electrochemical performance and high cycling stability.[118] Acetonitrile (ACN) is an important oxidation-tolerant organic solvent with high ionic conductivity. Despite its poor reduced stability, ACN-based HCEs can form stable SEI to show excellent cycling performance.[119] ACN-based LHCEs electrolytes show limited solubility of LiPS, leading to an excellent CE and improved capacity retention. In LHCEs, TTE has been demonstrated to participate in the reactions with both electrodes to form passivated films that prevent parasitic reactions and therefore improve utilization of active material and CE through mitigating LiPS dissolution and boosting conversion kinetics from polysulfides to Li_2S/Li_2S_2.[120,121]

Because of the high solubility of LiPS in ether electrolytes, use of novel solvents with less LiPS solubility is a practically feasible method to boost Li–S performance. A suitable choice is ionic liquid (IL), which has low solubility for LiPS. For example, LiPS has poor solubility in solvated ILs, which leads to high CE and a longer cycle life in Li–S batteries.[122] Compared with the 30% self-discharge rate in ether-based electrolytes, a battery using a $LiNO_3$-containing [PP13][TFSI]-based electrolyte shows zero self-discharge because the weak Lewis acid/basic properties of the [PP13][TFSI] inhibit the dissolution of LiPS.[123] Use of weakly solvated solvents can suppress LiPS solubility to improve cycling stability. There is poor solubility with LiPS in the DOL/DME

electrolyte with low polar methyl propyl ether (MPE) as a co-solvent.[124] Li–S batteries using a DOL/DME/MPE electrolyte show improved cycling stability, with a capacity retention of 71.5% following 200 cycles and a high average CE of 99.44%, which is significantly greater than those of the conventional DOL/DME electrolyte of, respectively, 46.9% and 98.06%, Figure 6A,B. In low polar diethyl ether electrolytes, there is also lower solubility of LiPS, leading to improved electrochemical performance.[37] However, blindly reducing the solubility of LiPS will not boost the electrochemical performance. Compared with SL (donor number [DN] = 14.8) and DOL/DME (DME, DN = 20; DOL, DN = 17), dimethyl sulfoxide (DMSO) with greater DN (DN = 30) exerts a strong solvation effect of Li^+ and high solubility for LiPS, resulting in greater nucleation overpotential and a significant shuttle effect in the DMSO electrolyte.[126] In an SL electrolyte with low DN, the poor conductively discharged product Li_2S_x with less solubility would precipitate, and break away from the conductive network leading to poor active materials utilization. For DOL/DME with intermediate DN numbers, LiPS shows proper solubility, balancing nucleation of the Li_2S_x particles and the solubility of LiPS, leading to better discharge capacity. Therefore, proper solubility for LiPS is important for Li–S cells to boost the utilization of active materials.

Additionally, electron-insulated Li_2S/Li_2S_2 is insoluble in the electrolyte, leading to poor capacity retention.[127] Following long cycling, volume expansion of the S cathode will destroy the integrity of the cathode and cause Li_2S/Li_2S_2 to detach from the conductive network, which decreases the utilization of active materials and drastically reduces the discharge capacity. A practical alternative method to solve this is to make Li_2S/Li_2S_2 soluble, increasing the utilization of active materials. Deep eutectic solvents (DESs) consisting

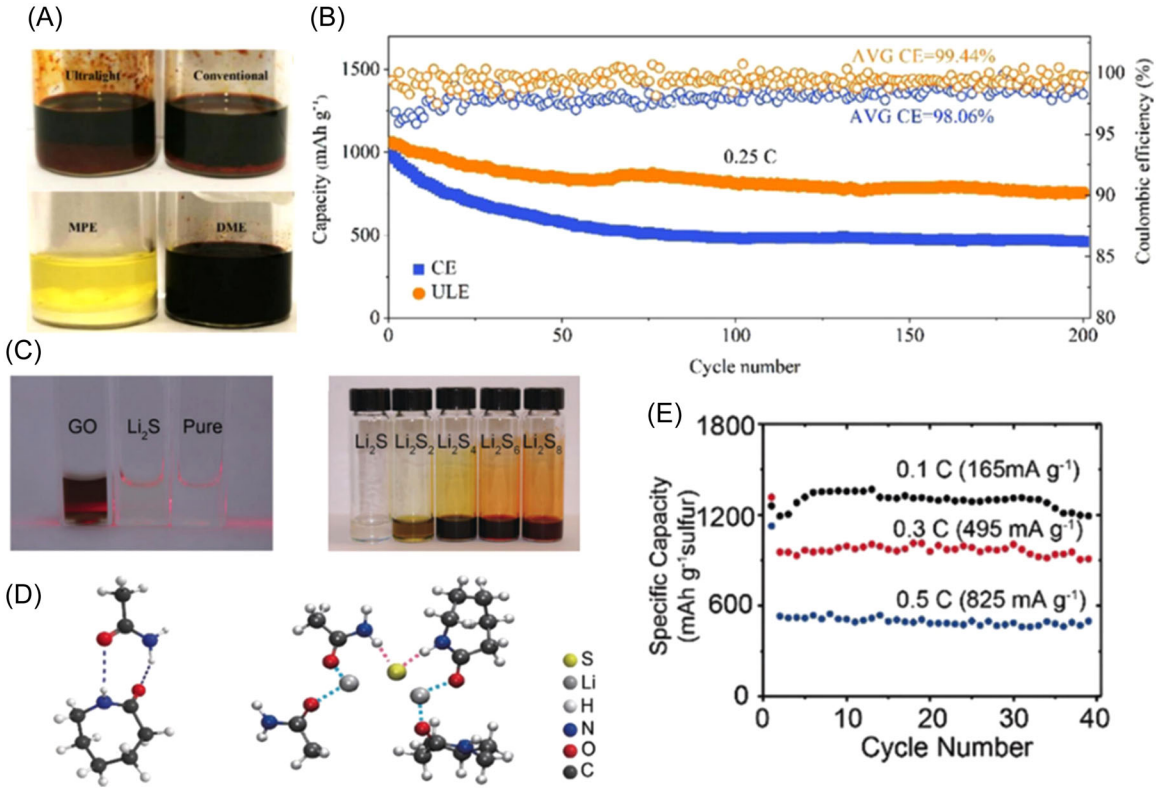

FIGURE 6 (A) Comparison of the solubility for LiPS in methyl propyl ether (MPE) and DME. Reproduced with permission.[124] Copyright 2021, Wiley-VCH. (B) Cycling stability for the cathode in an electrolyte (conventional electrolyte: 1 mol/L LiTFSI DME/DOL (1:1, volume ratio) + 2 wt% $LiNO_3$, ultralight electrolyte: 0.4 mol/L $LiNO_3$ + 0.2 mol/L LiTFSI, DME/MPE (48:52, volume ratio). Reproduced with permission.[124] Copyright 2021, Wiley-VCH. (C) Tyndall test showing no precipitation or colloids in 0.4 mol/L Li_2S/CPL/acetamide solution. Pure CPL/acetamide and GO dispersion used as control samples (left), and photograph showing dissolution of polysulfides and sulfide in CPL/acetamide. The concentration of S is 0.4 mol/L in all samples (right). Reproduced with permission.[125] Copyright 2019, Wiley-VCH. (D) CPL/acetamide mixture bound by an intermolecular hydrogen bond (left). A hypothetical dynamic solvation structure that involves multiple solvent molecules to dissolve Li_2S (right). Reproduced with permission.[125] Copyright 2019, Wiley-VCH. (E) Cycling performance of 0.2 mol/L Li_2S in the DES electrolyte for Li–S batteries. Reproduced with permission.[125] Copyright 2019, Wiley-VCH. CPL, caprolactam; DES, deep eutectic solution; DME, dimethoxyethane; DOL, dioxolane; LiPS, lithium polysulfide.

of caprolactam (CPL) and acetamide show the dissociation of Li_2S because of the strong interaction(s) between S^{2-} and amide hydrogen (N–H) and between Li^+ and carbonyl oxygen in the DES, as is shown in Figure 6C,D. Li–S batteries with this "new" electrolyte show a capacity of 1360 mAh/g at 0.1 C with 94.8% capacity retention following 40 cycles, Figure 6E.[125] DES electrolytes are safe and low cost, which represent major advantages in large-scale applications. However, DES can dissolve metal oxide;[128] therefore, it can cause the dissolution of the current collector, leading to reduced cycling stability.

Because the selection of cathodes impacts the lifespan of batteries, there needs to be different focus for future research application. For high-voltage cathodes, Al corrosion and CEI decomposition will require increased attention. Additional methods will need to be developed to prevent the shuttle effect in Li–S batteries.

3 | ACHIEVING FAST CHARGE

In LMBs, charge transfer at the Li anode can be conveniently divided into the following steps: (1) Li^+ transfers from the cathode to the anode in the electrical field, (2) Li^+ de-solvates at the anode surface, and (3) de-solvated Li^+ receives electrons and forms Li. The electrochemical reaction rate is controlled by concentration polarization, Step 1, and electrochemical polarization, Steps 2 and 3, as shown in Figure 7A.[23] Because electron transfer is fast, rapid Li^+ transport and facile de-solvation are key to achieving fast charge in LMBs.[131]

3.1 | High ion conductivity

High ion conductivity is a prerequisite for fast charge. Many simple Li salts, for example, Li_2O, LiCl, and LiF, have limited solubility in nonaqueous solvents, because of which high ion conductivity cannot be achieved. $LiPF_6$ has low dissociation energy and good solubility in carbonate solvents, resulting in good ionic conductivities at ambient temperature, for example, 10.8 mS/cm for 1 mol/L $LiPF_6$ EC/DMC at 25°C. However, chemically unstable $LiPF_6$ will hydrolyze at a moderate temperature in the presence of trace protic impurities (e.g., water and alcohol).[101] Fluorinated sulfonimide salts LiFSI and LiTFSI, which include a highly conjugated anionic center ($–SO_2–N^–SO_2–$), are generally well dissociated

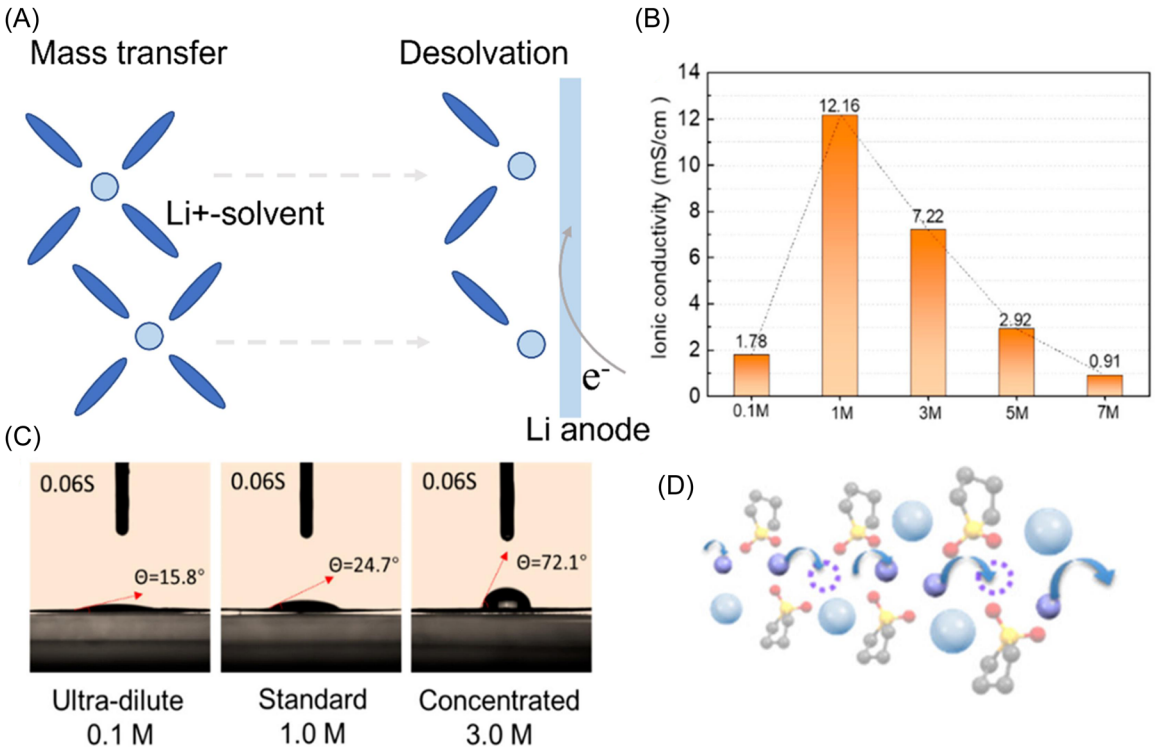

FIGURE 7 (A) Schematic showing three steps for charge transfer at the Li anode. (B) Ionic conductivity of 0.1, 1, 2, 3, and 5 mol/L DOL/DME-based electrolyte. Reproduced with permission.[120] Copyright 2020, American Chemical Society. (C) Digital photograph of different molarity electrolyte droplet contact angles on the S cathode. Reproduced with permission.[129] Copyright 2020, American Chemical Society. (D) Hopping mechanism in the SL electrolyte. Color code: Li = purple; oxygen = red; carbon = gray; anion = light blue; and sulfur = yellow. Reproduced with permission.[130] Copyright 2019, American Chemical Society. DME, dimethoxyethane; DOL, dioxolane.

and soluble in organic solvents, showing adequate ionic conductivity of 12.16 mS/cm for 1 mol/L LiTFSI DOL/DME at 25°C, high thermal stability, and resistance toward hydrolysis. However, LiTFSI-based electrolytes are corrosive toward Al current collectors, leading to poor cycling stability. Given the cost and electrochemical performance, $LiPF_6$ is the "first choice" in many commercial LIBs. Solvents need to have a high ε to sufficiently dissociate Li salts to form SSIP and free anions to yield high ionic conductivity. Therefore, the ion conductivity of an aqueous electrolyte is greater than that of a nonaqueous electrolyte because of the greater ε for water. Designed electrolytes should have low viscosity to facilitate ion transport. Compared with other solvents, carbonate and ether solvents have low viscosity for rapid ion transport and greater ε for dissociation of Li salts. Therefore, these are used widely in practical research.[26] The viscosity of HCEs is greater than that for commonly used electrolytes (1 mol/L), leading to lower ion conductivity, Figure 7B. Although less Li salt dissolved in electrolyte provides lower ion conductivity, dilute electrolytes, including 0.1 mol/L LiTFSI in DOL/DME, show required ion transport in LMBs.[129] The 0.1 mol/L LiTFSI DOL/DME electrolyte with low viscosity and excellent wetting on sulfur cathodes (Figure 7C) shows significantly greater rate capability and better cell stability than the standard 1 mol/L electrolyte. However, many SSIPs in dilute electrolytes cannot generate anion-derived SEI; fewer Li^+ ions easily induce a concentration gradient and accelerate the growth of dendrites.

3.2 | High Li^+ transference number

Charge transfer is accomplished via transport of Li^+ and anions in electrolytes. Because of differing radii, cations and anions have different transport rates, leading to different transference numbers for cations and anions. A smaller ionic radius for Li^+ exerts strong Coulombic attraction toward solvent molecules, leading to a solvation sheath around Li^+ ions. Therefore, Li^+ always migrates with a solvation sheath, causing sluggish Li^+ transport.[26] Current liquid electrolytes usually have a Li transference number (t_{Li+}) < 0.5. In HCEs, despite high viscosity, fewer SSIPs lead to a high $t_{Li+} = 0.73$.[118] In SL-based HCEs, where two oxygen atoms of the sulfonyl group coordinate with two neighboring Li^+ and $TFSI^-$ to form ionic clusters, as shown in Figure 7D, Li^+ shows a hopping diffusion mechanism in which Li^+ are transferred from one coordinating site (on either SL or anions) to another vacant site through ligand exchange in the labile Li^+ coordination chains. Therefore, there is a high $t_{Li+} = 0.5$ in the SL electrolyte.[130] Despite the wide electrochemical window and excellent thermal stability in IL electrolyte, the cations and anions in IL compete with Li^+/anions from electrolytes for charge transportation, resulting in a lower value of t_{Li+}. For zwitterionic, for example, a borate-type zwitterion–LiTFSI electrolyte[132], and pyrrolidinium zwitterionic[133], in which anion and cation groups are on the same monomer unit, ion transport of cations and anions in IL is limited, leading to a higher value of t_{Li+} compared with traditional IL. "Immobilizing" anions are used to improve t_{Li+}; however, this method is useful only in (quasi) solid-state electrolytes, or single ion-conductive electrolytes to yield a high t_{Li+}.[134,135] However, improving t_{Li+} in liquid electrolyte is a less researched field.

3.3 | Facile de-solvation for fast charge

The Li^+ will de-solvate at the anode surface, then Li^+ receive an electron and finish plating. The strong solvation effect in the electrolyte causes sluggish de-solvation and greater nucleation barrier, leading to greater overpotential and poor rate performance during charge/discharge.[126] However, in de-solvation research, a commonly used electrode is obtained by slurry coating on an Al current collector, which shows nonuniformity in density, porosity, and tortuosity, that impacts mass transport in the electrolyte. Therefore, it is difficult to understand the reason for improved performance is promoting mass transport or facilitating de-solvation. Use of a single-particle electrode in a three-electrode electrochemical cell can obviate the influence of mass transfer. The $TFSI^-$ anion preferentially solvates Li^+ rather than PF_6^-; however, this results in a lower Li^+ binding energy that provides for more facile de-solvation and faster interfacial kinetics. Exchange current densities are therefore ca. 100 greater in electrolytes containing the $TFSI^-$ anion compared with those containing PF_6^- alone. At a high rate, the sluggish interfacial kinetics cause poor rate performance in the $LiPF_6$ electrolyte of ~75 mAh/g at 10 C, compared with the LiTFSI + $LiPF_6$ electrolyte of ca. 125 mAh/g at 10 C.[136] Facile de-solvation is not directly related to ion conductivity. An ACN-based HCE with lower ionic conductivity than a dilute electrolyte allows ultrafast charging in Li||graphite half-cells because the Li binding energies decrease in HCEs, leading to facile de-solvation.[39]

Fast charge will be necessary for the anticipated future demand for EVs. Although high ion conductivity, a high t_{Li+}, and facile de-solvation are necessary for fast charge, the significant Li dendrites originating from greater current also represent a major challenge in fast

charging LMBs. Therefore, formation of a stable SEI is also a prerequisite for fast charge.

4 | ACHIEVING WIDE WORKING TEMPERATURE

Wide working temperatures represent an important parameter for advanced batteries. However, changes in temperature have a significant impact on ion transport and interfacial reaction kinetics, which impose strict design requirements for electrolytes.

4.1 | Achieving low-temperature electrolytes

Sluggish ion transport at low temperatures causes sluggish electrochemical kinetics, greater overpotential, and reduced electrochemical performance. At an ultralow temperature (<−20°C), electrolytes undergo a phase change from liquid to solid, reducing ion conductivity. Therefore, use of a solvent with a lower melting point (T_m) can increase ion conductivity at low temperatures to boost low-temperature electrochemical performance.[137,138]

4.1.1 | Antifreezing solvent and liquefied gas electrolyte

Carbonate and ether electrolytes are commonly selected for LMBs. Compared with ether electrolytes (DOL, $T_m = -95$°C; DME, $T_m = -58$°C), carbonate electrolytes show higher T_m (EC, $T_m = 34$°C; propylene carbonate, $T_m = -55$°C; ethyl methyl carbonate, $T_m = -55$°C), which is not beneficial for boosting low-temperature electrochemical performance.[139] Antifreeze solvents with lower T_m can improve ionic conductivity at low temperatures and boost the electrochemical performance.[37] Diethyl ether (DEE) has lower T_m (−117°C) and can maintain high ion conductivity at low temperatures. On use in LMBs with a high-loading sulfurized polyacrylonitrile cathode and an N/P capacity ratio of 1, batteries with a DEE electrolyte retain 84% and 76% of room-temperature (25°C, RT) capacity when cycled at, respectively, −40°C and −60°C. Liquefied gas shows ultralow viscosity and ultralow T_m, which makes it an ideal solvent for stable Li deposition at low temperature as shown in Figure 8A. With the use of liquified fluoromethane (FM) as an antifreezing solvent for low-temperature LMBs, no Li dendrites with a high CE of 97% can be practically achieved at 25°C in LMBs (Figure 8B) and improved capacity, Figure 8C,D.[140] There is low solubility of Li salt in liquefied gas solvents (0.2 mol/L LiTFSI in FM), resulting in lower ionic conductivity. With ACN and THF additives that can dissociate LiTFSI well, liquefied gas electrolytes show greater salt solubility (1.2 mol/L LiTFSI in ACN-FM) and excellent ionic conductivity of 5.8 mS/cm at −60°C and 4.8 mS/cm at −78°C.[92,141] Therefore, LMBs with 1.2 mol/L LiTFSI–AN–FM electrolyte can deposit at −60°C with a high CE of 98.4% without dendrites. Using 1,1,1,2-tetrafluoroethane and pentafluoroethane as safe liquefied gases, the electrolyte maintains >3 mS/cm ionic conductivity from −78°C to 80°C.[142]

4.1.2 | Facile de-solvation boosts low-temperature performance

Although traditional ether electrolytes show high ion conductivity at low temperatures, they do not show better performance at low temperatures. For example, at temperatures below 0°C, there is a large Li nucleation barrier and an uneven Li deposition in the DOL/DME electrolyte.[143] This reported finding indicates that the low-temperature design of battery systems is more complex than simply ensuring an electrolyte with adequate ionic conductivity at low temperatures. At low temperatures, a strong de-solvation barrier becomes the rate-limiting step, causing poor Li deposition dynamics, as shown in Figure 9A.[145] Therefore, it is practically significant to facilitate Li^+ de-solvation at low temperatures.

Because solvents directly govern the de-solvation energy, selection of a solvent with low T_m and weakly solvated power leads to stable Li deposition at low temperatures. In DEE with low T_m (−116°C), Raman spectra and MD findings show that significant AGGs exist in the DEE electrolyte, confirming that DEE is a solvent with weak solvated ability.[37] In contrast, the DOL/DME electrolyte shows strong interaction between the solvent and Li^+. A stronger de-solvated barrier in the DOL/DME electrolyte increases the local charge-transfer impedance, leading to poor low-temperature electrochemical performance. The DEE-based electrolyte shows lower de-solvation energy, facilitating interface reaction kinetics. There is a high CE in coin cells with a DEE-based electrolyte at low temperatures. Dimethoxymethane (DMM) shows the anomeric effect, which thermodynamically favors a gauche–gauche conformation that cannot chelate Li^+, leading to weak solvated ability, as shown in Figure 9B,C.[146] Lower de-solvation

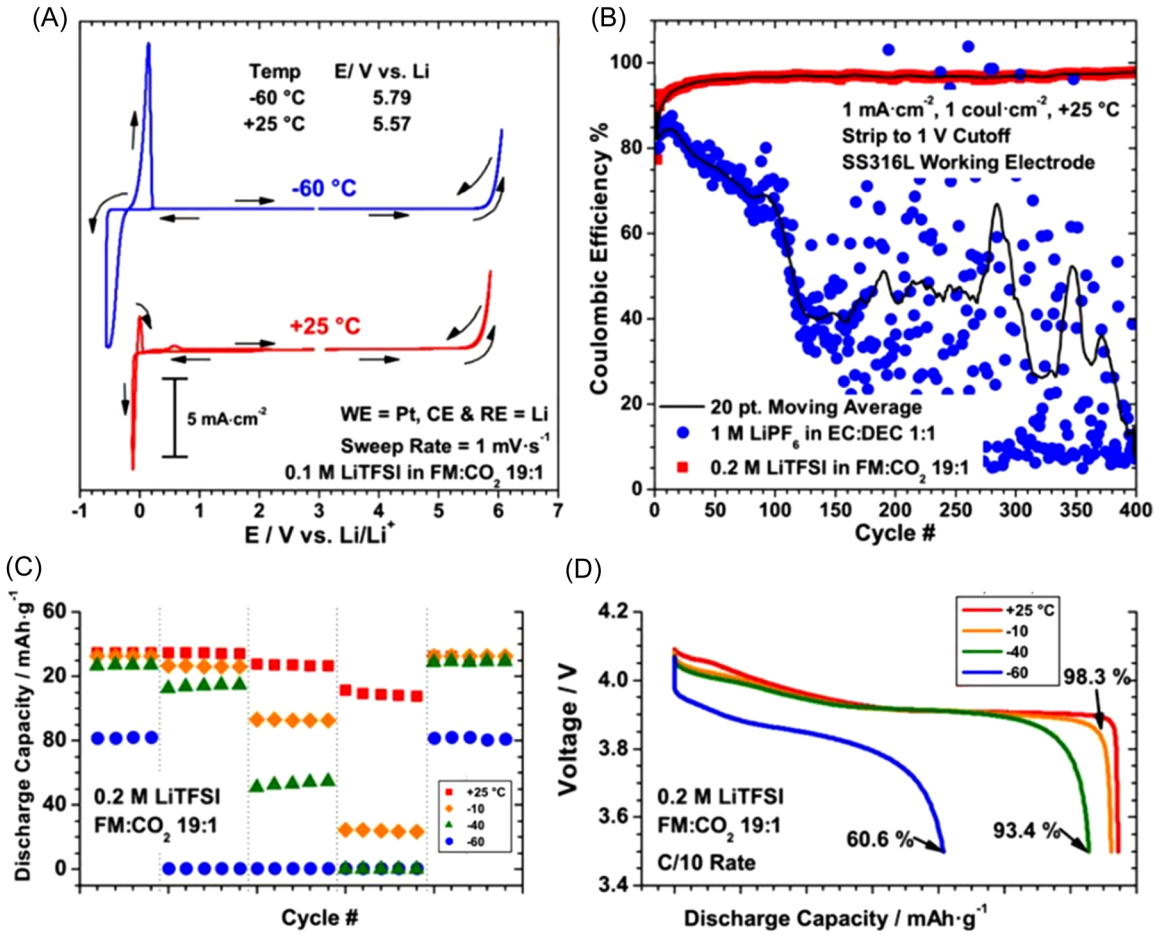

FIGURE 8 (A) Cyclic voltammetry curves for 0.1 mol/L LiTFSI in FM at 25°C and −60°C. (B) CE for Li plating/stripping over 400 cycles using FM- and conventional liquid-based electrolytes at 25°C. (C) Discharge capacity at different temperatures and C values. (D) Voltage versus discharge capacity at different temperatures at 0.1 C. Reproduced with permission.[140] Copyright 2017, Science. CE, Coulombic efficiency; FM, fluoromethane.

energy promotes more uniform Li deposition and high plating/stripping efficiency in the DMM electrolyte at low temperatures, as shown in Figure 9D.[144]

Additionally, a reported method to facilitate de-solvation at low temperatures involves the use of LHCEs.[147] With LHCEs, the inert co-solvent usually has low ε that cannot influence the Li^+ solvation environment in HCEs. In solvents with high ε, highly polar molecules boost the dipole–dipole force, leading to high T_m. Use of an inert dilute co-solvent breaks the strong interaction between the highly polar molecules and decreases the T_m value for the electrolyte, widening the liquid-phase range. CIPs and AGGs in LHCEs promote facile de-solvation and generate anion-derived SEI. Therefore, LHCEs show excellent low-temperature electrochemical performance. 4.2 mol/L LiFSI-FEC/methyl(2,2,2-trifluoroethyl) carbonate (FEMC) dissolves in diluted solvent 1,1,2,2-tetrafluoro-1-(2,2,2-trifluoroethoxy)ethane (D2), forming 1.28 mol/L LiFSI in FEC/FEMC/D2 with wide liquid range from −125°C to 70°C. This electrolyte shows high ion conductivity of $>1 \times 10^{-2}$ mS/cm at −80°C.[36] Based on quantum chemistry computations, introduction of FEC/FEMC into a nonpolar solvent D2 reduces the solvation energy. Therefore, there is better electrochemical performance at low temperatures. Other LHCEs also show better low-temperature performance; for example, LMBs with SL-based LHCEs can cycle at −10°C.[90]

4.2 | Designed high-temperature electrolyte

Traditional ether and carbonate electrolytes are volatile, leading to high pressure inside batteries cycled at high temperatures. Long cycles at high temperatures cause battery expansion and even explosion. Therefore, selected nonvolatile solvents have been reported as electrolytes for LMBs at high temperatures.

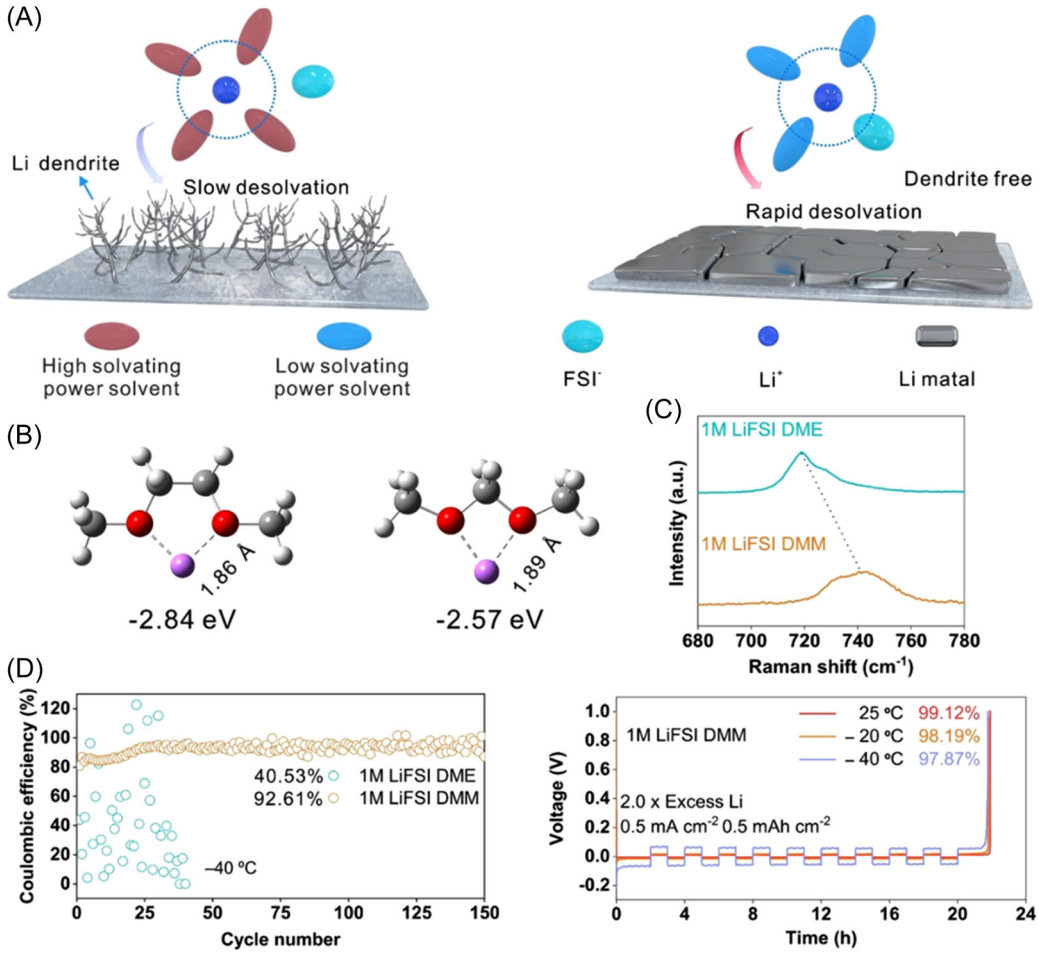

FIGURE 9 (A) Illustration of the relationship between Li deposition morphology and solvated ability of solvents at low temperatures. (B) Binding energies of the Li^+–solvent complex. left: Li^+–DME; right: Li^+–DMM. (C) Raman spectra of DMM and DME electrolytes. (D) Plating/stripping profile for CE determination in 1 mol/L LiFSI DME and 1 mol/L LiFSI DMM at 0.25 mA/cm^2 at −40°C, and Aurbach CE tests of the DMM electrolyte at various temperatures. Reproduced with permission.[144] Copyright 2022, Wiley-VCH. CE, Coulombic efficiency; DME, dimethoxyethane; DMM, dimethoxymethane.

ILs with nonvolatility and high thermal stability are highly suitable for high-temperature LMBs.[16] For example, the phosphonium IL trihexyldecylphosphonium bis (trifluoromethanesulfonyl)imide/1.6 mol/L LiTFSI electrolyte has a high anodic stability of 5 V (vs. Li^+/Li) at 100°C together with stable cycling stability.[148] High temperature decreases the viscosity of the IL electrolyte, promoting ion conductivity. The DESs are also not volatile and have good thermal stability. The Li||$LiMn_2O_4$ cell with a LiTFSI/N-methylacetamide/FEC-based DES polymer electrolyte showed a capacity retention of 86.1% following 200 cycles at 0.2 C and satisfactory cycling stability at elevated temperatures.[149] Although IL and DES electrolytes are advantageous, including wide electrochemical window and high thermal stability, these do not stabilize the Li anode to promote stable Li deposition and lead to poor cycling stability. The high viscosity also limits application in LMBs.

4.3 | Designed wide working temperature electrolyte

Synthesis of an electrolyte with wide working temperature is practically difficult because the electrolyte should not only have wide liquid range but also mitigate the impact caused by high and low temperatures on SEI/CEI. Several methods have been reported for achieving LMBs with wide working temperature.

4.3.1 | Liquefied gas electrolytes for wide temperature ranges

Because liquefied gases use pressurized hermetically sealed cells, they maintain the liquid phase at high temperatures. Liquefied gas electrolytes show excellent conductivity of >4 mS/cm over a temperature range of −78°C to 75°C,

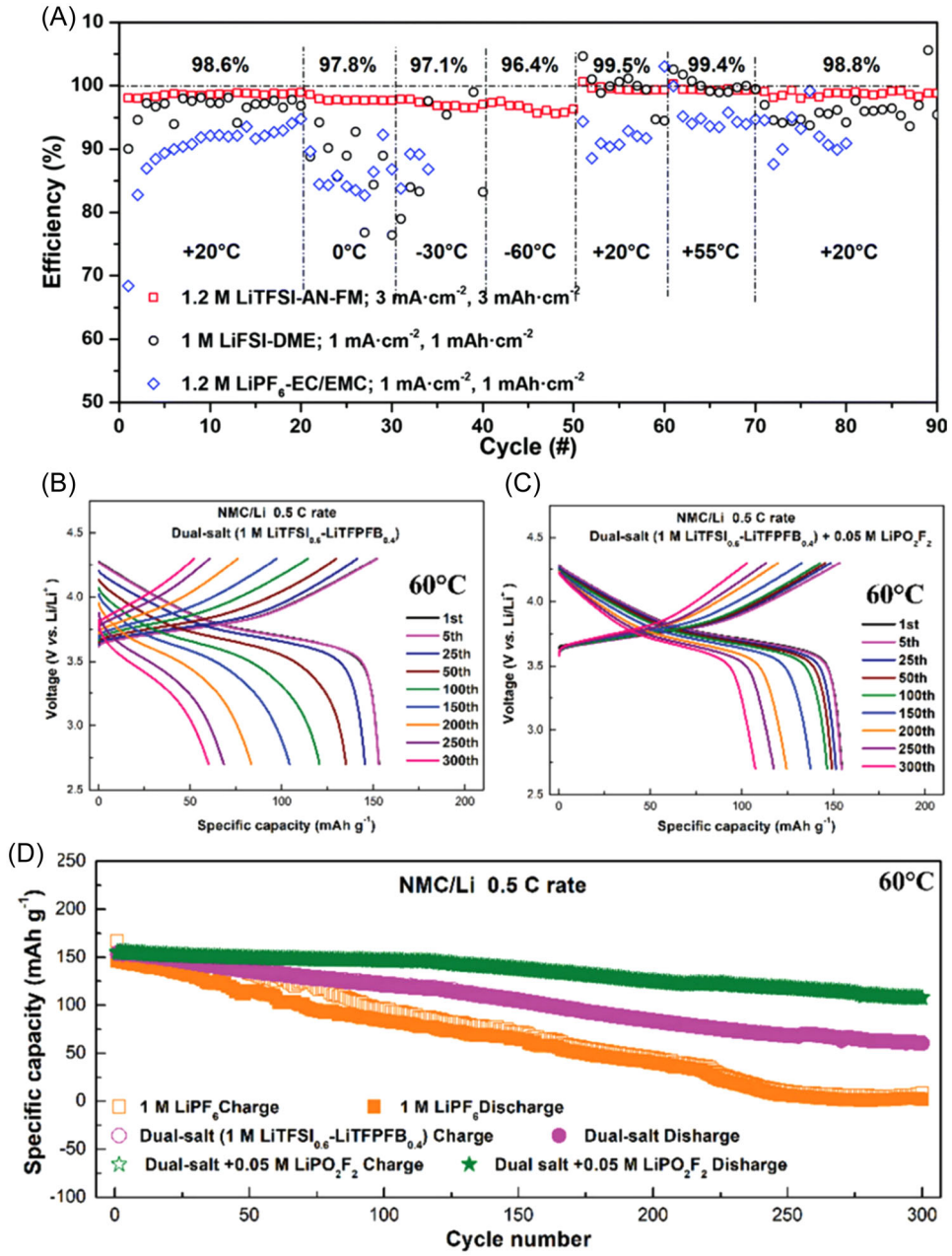

FIGURE 10 (A) Coulombic efficiency of Li deposition using 1.2 mol/L LiFSI AN-FM liquified gas electrolyte at various temperatures. Reproduced with permission.[141] Copyright 2020, Royal Society of Chemistry. Charge/discharge curve for Li||NCM batteries using (B) dual-salt and (C) 0.05 mol/L $LiPO_2F_2$-added dual-salt electrolyte. Reproduced with permission.[150] Copyright 2019, Wiley-VCH. (D) Cycling performance for Li||NCM batteries (2.7–4.3 V) with 1 mol/L $LiPF_6$-based electrolyte and 1 mol/L LiTFSI (0.6) + LiTFPFB (0.4) dual-salt electrolyte with and without 0.05 mol/L $LiPO_2F_2$ additive, respectively, at 60°C at 0.5 C. Reproduced with permission.[150] Copyright 2019, Wiley-VCH. DME, dimethoxyethane; EC, ethylene carbonate; FM, fluoromethane.

leading to a high CE of 99.4% and stable cycling of 4.5 V (vs. Li^+/Li) LMBs in the temperature range of 55°C to −60°C, as shown in Figure 10A.[141] Liquefied 1,1,1,2-tetrafluoroethane and pentafluoroethane electrolytes show stable cycling of Li|| NMC622 batteries from −60°C to 55°C.[142] However, liquefied gas electrolytes are only suitable for special needs because pressurized hermetically sealed cells increase the cost significantly and decrease portability and flexibility.

4.3.2 | LHCEs for wide operating temperature

LHCEs show facile de-solvation at low temperatures and modify the solvation structure of Li^+ to generate inorganic-enriched SEI, which maintains stability at high temperatures. Therefore, LHCEs are practically suitable for LMBs with wide working temperature. LHCE

(1.28 mol/L LiFSI in FEC/FEMC/D2) shows high ionic conductivity in the temperature range −125°C to 70°C.[36] The Li||$LiNi_{0.8}Co_{0.15}Al_{0.05}O_2$ battery using D2-LHCEs at −85°C shows 56% of RT capacity. The LHCE of 1.4 mol/L LiFSI in DMC/EC/TTE enables NCM811-based LIBs to show excellent cycling stability at RT and 60°C, good rate capability under fast charging and discharging up to 3 C, and superior low-temperature discharge performance down to −30°C with a capacity retention of 85.6% at 0.2 C.[151] Although the addition of dilute hydrofluoroether solvents decreases the viscosity and T_m for electrolytes and facilitates anion-derived SEI formation, volatile hydrofluoroethers limit the ultrahigh temperature (>100°C) performance of LHCEs.

4.3.3 | Additives for electrolytes with wide working temperature

A change of temperature impacts SEI/CEI. The organic component in SEI/CEI is not stable and decomposes at elevated temperatures, creating a porous SEI/CEI layer instead of a film SEI/CEI coated on the electrode surface that exposes more lithium/cathode material to the electrolyte and leads to electrolyte decomposition.[152,153] Low temperatures cause uneven deposited Li morphology and a rough surface of the Li anode, leading to unstable CE.[143,145] Therefore, synthesis of stable SEI/CEI is important for practical achievement of LMBs with low, high, and wide operating temperature. Use of additives is a practically useful method to synthesize stable SEI/CEI to obtain LMBs with wide working temperature. Li–S batteries with FEC as additives in 6.5 mol/L LiTFSI electrolyte show outstanding cycle performance over temperatures ranging from −10°C to 90°C.[154] This superior battery performance is attributed to the LiF-rich SEI formed on the Li metal anode that suppresses the continuous growth of Li dendrites. Carbonate electrolyte containing a $LiPO_2F_2$ additive shows low T_m and high boiling point and improved cycle ability and rate capability over the temperature range of −40°C to 90°C.[150] FEC and lithium difluorobis(oxalato) phosphate (LiDFOP),[155] lithium oxalyldifluoroborate (LiODFB),[156] LiDFBOP,[157,158] and LiBOB[159,160] can boost electrochemical performance over a wide temperature range as shown in Figure 10B–D. Table 2 presents a comparison summary of selected LMBs working at various temperatures.

In future design of LMBs with low, high, and wide working temperature, in addition to the electrolyte, other factors should also be considered, such as the cathode, lithium salt, additives, separator, and binder. Because these will all influence battery performance, a change in temperature will magnify the effects and impact the electrochemical performance and lifespan.

5 | IMPROVING ENERGY DENSITY

Energy density is dependent on the capacity and the operational voltage. Currently, the method used to practically improve energy density is to increase the electrode capacity but boost the cut-off voltage to widen operational voltage window, which can also improve the energy density.[161,162] For example, boosting the cut-off voltage of the $LiCoO_2$ cathode to 4.6 V (vs. Li^+/Li) leads to a ca. 40% improvement in the specific energy density.[163] However, current traditional electrolytes with lower anodic stability (1 mol/L $LiPF_6$ in EC ~4.3 V vs. Li^+/Li, 1 mol/L LiTFSI in DOL/DME < 4.0 V vs. Li^+/Li) are not suitable for high voltage cathode, limiting any further increase in energy density. There are several methods to improve the anodic voltage of electrolytes.

5.1 | High anodic stability solvents

The electrochemical window for solvents govern the operational range of electrolytes. Therefore, replacing ether and carbonate solvents with solvents of intrinsic wide electrochemical window improves the anodic stability of electrolytes. The sulfonyl group with strong electron-withdrawing ability shows low HOMO, boosting oxidation stability; therefore, sulfone solvents show greater anodic stability.[26,164] Sulfonamide-based electrolytes show higher anodic voltage of >4.7 V (vs. Li^+/Li). $LiCoO_2$ cathodes with this electrolyte retain, respectively, 89% and 85% of capacity following 200 and 100 cycles at cut-off voltages of 4.55 V (vs. Li^+/Li) and 4.6 V (vs. Li^+/Li).[165] The 1 mol/L LiFSI/N,N-dimethyltrifluoromethane-sulfonamide (DMTMSA) electrolyte enables stable cycling of NCM811 cathodes at 4.7 V (vs. Li^+/Li) with a high specific capacity of >230 mAh/g and an average CE of >99.65% over 100 cycles.[166] Fluorinated sulfone solvents are also synthesized for high-voltage cathodes.[167] Following fluorination, the sulfone solvents have excellent anodic stability of >6.0 V (vs. Li^+/Li).[168] However, fluorination leads to lower solubility of Li salt and lower ion conductivity; the use of a co-solvent to dissociate Li salts will decrease the anodic stability. Therefore, the high solubility of Li salt in high anodic stability solvents is important. SL with high voltage stability of >5.0 V (vs. Li^+/Li) leads to high solubility of Li salt, which makes it a suitable choice for high-voltage electrolytes.[49] The 1 mol/L LiFSI SL-based electrolyte shows a high decomposition voltage of >5 V (vs. Li^+/Li)

TABLE 2 Comparison of reported LMBs working at various temperatures.

Electrolyte	Electrode	Temperature (°C)	Capacity (mAh/g)
1.28 mol/L LiFSI FEMC/FEC/D2 (1:2:7, volume ratio)[36]	$LiNi_{0.8}Co_{0.15}Al_{0.05}O_2$	70, −85	170 at 70°C (1/3 C) 96 at −85°C (1/3 C)
1.2 mol/L LiTFSI AN/FM (1.2:1, weight ratio)[141]	NCM622	55, −20	200 after 50 cycles at 55°C (0.5 C) 110 after 300 cycles at −20°C (1/3 C)
6.5 mol/L LiTFSI FEC[154]	Sulfur	90, −10	981 after 50 cycles at 90°C (1 C) 453 after 50 cycles at −10°C (0.1 C)
0.6 mol/L LiTFSI + 0.4 mol/L LiTFPFB + 0.05 mol/L $LiPO_2F_2$ PC/EC/EMC (1:1:3, weight ratio)[150]	NCM811	80, −20	100 after 300 cycles at 60°C (0.5 C) 101 after 50 cycles at −20°C (0.1 C)
0.8 mol/L LiTFSI + 0.2 mol/L LiODFB ADN/EC (AE) (1:1, volume ratio)[156]	LTO	150, −20	150 after 100 cycles at 150°C (1 C) 120 after 100 cycles at −20°C (1 C)
5 mol/L LiTFSI EA/SL (7:3, volume ratio) TTE[147]	NCM523	25, −40	200 at 25°C (0.1 C) 91 after 200 cycles at −40°C (1 C)
LiFSI-SL-TTE (1:3:3, molar ratio)[90]	NCM111	25, −10	140 after 20 cycles at 25°C (0.1 C) 110 after 10 cycles at −10°C (0.2 C)
1 mol/L LiFSI DEE[37]	SPAN	23, −60	300 after 50 cycles at 23°C (1/3 C) 230 after 50 cycles at −60°C (0.2 C)
1.4 mol/L LiFSI DMC/EC/BTFE (2:0.2:3, molar ratio)[151]	NCM811	25, 60	175 after 600 cycles at 25°C (1/3 C) 180 after 100 cycles at 60°C (1/3 C)
1 mol/L LiFSI DMM[144]	LTO	25, −20	130 after 200 cycles at 25°C (0.5 C) 130 after 100 cycle at −20°C (0.5 C)

Abbreviation: LMB, lithium metal battery.

as shown in Figure 11A, improving cycling stability and capacity retention in the graphite||$LiNi_{0.5}Mn_{1.5}O_4$ full cell.[49]

ILs and DESs with wide electrochemical window are suitable for high-voltage electrolytes. Piperidinium and pyrrolidinium ILs possess a high anodic stability of >5.5 V (vs. Li^+/Li).[170,171] Solvated IL obtained by directly mixing tetra(ethylene glycol) dimethyl ether with LiTFSI (1:1, molar ratio) has higher anodic stability of 5 V (vs. Li^+/Li) as shown in Figure 11B because of the donation of lone pairs of ether oxygen atoms to the Li^+ cation, resulting in the decrease of the HOMO energy level of a glyme molecule.[169] For dual-anion DES based on succinonitrile (SN) and LiTFSI/LiDFOB, no apparent redox peaks are detected in the range 0–5 V (vs. Li^+/Li), indicating its wide electrochemical window.[172] Table 3 presents the oxidation stability and electrochemical performance of selected electrolytes. However, these solvents have high viscosity, resulting in poor ion conductivity and reduced wettability toward electrodes and separators. For phosphate solvents, ILs, and DES, the reduced ability to form stable SEI limits large-scale application. The high viscosity of these solvents also leads to poor electrochemical performance.

Introduction of F into an ester or ether results in a decrease in energy levels for both HOMO and the LUMO. The lower HOMO leads to higher resistance against oxidation.[26] The fluorinated DTDL electrolyte shows high oxidation stability up to 5.5 V (vs. Li^+/Li) as shown in Figure 11C.[61] Following fluorination, the FDMB electrolyte shows higher oxidation stability of >6 V (vs. Li^+/Li) compared with 4 V (vs. Li^+/Li) for the DME-based electrolyte.

5.2 | HCEs for high anodic stability

HCEs can boost anodic stability, and likely the best example is the "water in salt" electrolyte, which expands the narrow electrochemical window of the aqueous electrolyte (1.23 V) to >3.0 V.[177] Following solvation with Li^+, HOMO of the solvent molecules decreases, leading to stronger resistance against oxidation.

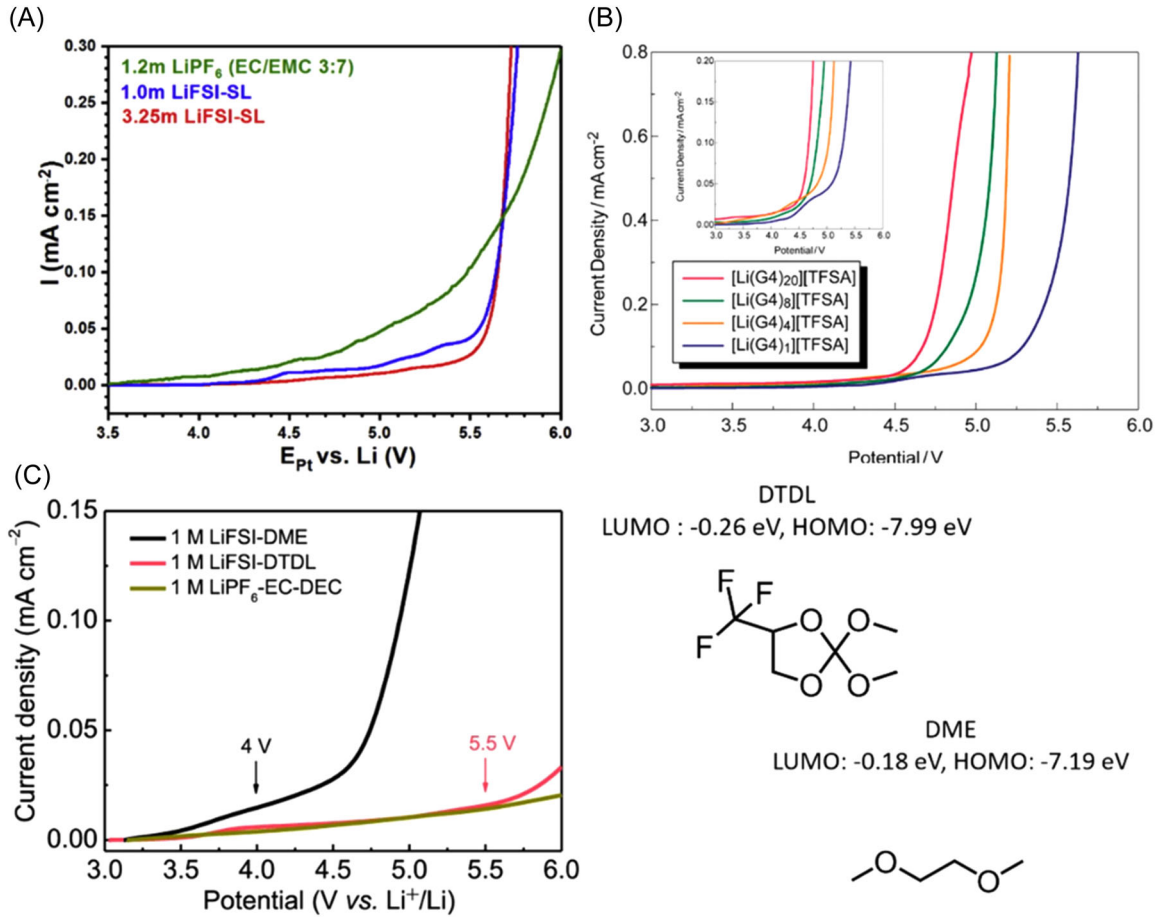

FIGURE 11 (A) Electrochemical stability of the SL electrolyte. Reproduced with permission.[49] Copyright 2019, Elsevier. (B) Linear sweep voltammogram (LSV) for $[Li(G_4)_x][TFSI]$. Reproduced with permission.[169] Copyright 2011, American Chemical Society. (C) Oxidation stability of the DTDL electrolyte via LSV, and LUMO and HOMO. Reproduced with permission.[61] Copyright 2022, Springer Nature. DEC, diethyl carbonate; DME, dimethoxyethane; EC, ethylene carbonate; HOMO, highest occupied molecular orbital; LOMO, lowest unoccupied molecular orbital; SL, sulfolane.

However, with common electrolytes (1 mol/L), free solvent molecules are predominant and there is limited improvement in oxidation stability. With an increase in the salt concentration, the amount of free solvent molecules decreases, leading to high oxidation stability. The concept of "solvent in salt" in various organic solvents, including carbonate[48] and ether,[118] confirms that high salt concentrations can practically boost oxidation stability.[90] Additionally, in LHCE, because diluted solvent also show high anodic stability, LHCEs maintains stability against oxidation.[90,176]

6 | IMPROVING THE SAFETY OF LMBs

Low risk and high safety are design prerequisites for LMBs. Common risks in LMBs are caused by gas evolution and thermal runaway.[178]

6.1 | Gas evolution mechanism

Gas evolution occurs due to oxygen release from cathode materials and decomposition of the electrolyte.[179] A high degree of delithiation at high voltage causes structural destruction; then, lattice oxygen release accelerates chemically oxides electrolytes. Electrolyte decomposition at the electrode is the main reason for gas evolution. In the anode, EC, which is the carbonated electrolyte that is used the most, is reduced via a one-electron ring-opening reaction to form a lithium alkyl carbonate radical that dimerizes to form lithium ethylene decarbonate and releases ethylene gas, Figure 12A.[180] The reduction of DMC proceeds via a one-electron reaction forming a lithium alkyl carbonate radical that decomposes into lithium methyl carbonate (LMC) and ethane gas, Figure 12A. LMC can react in two ways: it can (1) decompose to release CO_2 gas and form lithium methoxide and (2) react with water to form a mixture

TABLE 3 Oxidation stability and electrochemical performance of selected electrolytes.

Electrolyte	Oxidation stability (Li^+/Li)	Electrode and cut-off voltage (Li^+/Li)	Capacity retention
1 mol/L LiFSI $DMCF_3SA$[165]	~5 V	Li||$LiCoO_2$, 4.6 V	85% after 100 cycles
1.2 mol/L LiFSI F5DEE[32]	~4.6 V	Li||NCM, 4.4 V	80% after 270 cycles
7 mol/L LiFSI FEC[53]	5 V	Li||$LiNi_{0.5}Mn_{1.5}O_4$, 5 V	78% after 130 cycles
1 mol/L LiFSI DTDL[61]	5.5 V	Li||NCM811, 4.3 V	84% after 200 cycles
4 mol/L LiFSI DEE[31]	5 V	Li||NCM811, 4.4 V	80% after 180 cycles
1 mol/L LiFSI FDMB[62]	5.2 V	Li||NCM532, 4.2 V	90% after 400 cycles
0.95 mol/L LiFSI TFEP FEMC (1:3, volume ratio)[173]	4.9 V	Li||$LiNi_{0.5}Mn_{1.5}O_4$, 4.9 V	70% after 200 cycles
1 mol/L LiFSI DME FEO (1:9, weight ratio)[174]	~5 V	Li||NCM811, 4.4 V	80% after 300 cycles
LiFSI: SN (1:3.3, weight ratio) + 0.03 mol/L LiDFOB[172]	>5 V	Li||$LiCoO_2$, 4.7 V	70% after 500 cycles
3.25 mol/L LiTFSI SL + 0.1 mol/L $LiNO_3$	5.2 V	Li||NCM811, 4.4 V	99.5% after 200 cycles
1 mol/L $LiPF_6$ FEC/DME (3:7, volume ratio) + 0.65 mol/L $LiNO_3$[67]	4.4 V	Li||NCA, 4.3 V	59% after 160 cycles
1.2 mol/L LiFSI DMC/BTFE (1:1.5, molar ratio)[54]	5 V	Li||NCM111, 4.3 V	80% after 700 cycles
1 mol/L LiTFSI DEG-FTriEG[175]	5.4 V	Li||NCM811, 4.4 V	~60% after 100 cycles
LiFSI + DME + TTE (1:1.2:3, molar ratio)[176]	4.4 V	Li||NCM811, 4.4 V	80% after 155 cycles
1 mol/L $LiPF_6$ FEC/FEMC/TTE (2:6:2, weight ratio) + 2 wt% LiDFOB[106]	6.5 V	Li||$LiNiO_2$, 4.4 V	81% after 400 cycles
3.25 mol/L LiFSI SL[49]	5 V	Li||$LiNi_{0.5}Mn_{1.5}O_4$, 4.6 V	69% after 1000 cycles
1 mol/L LiDFTFSI EC/EMC (3:7, volume ratio)[101]	5.6 V	Li||NCM111, 4.2 V	87% after 200 cycles
1 mol/L $LiPF_6$ FEC/FEMC/TTE (2:6:2, weight ratio)[58]	6.5 V	Li||NCM811, 4.4 V	90% after 450 cycles

of carbonates, methanol, and CO_2. In the cathode, EC is chemically oxidized to CO_2 and glycolic acid, which is chemically oxidized again to form water and oxalic acid, as shown in Figure 12B. DMC is oxidized with a reactive oxygen species, for example, singlet O_2, to produce formic acid and LMC. LMC reacts further via hydrolysis or thermal decomposition to form formic acid, CO_2, and H_2O, Figure 12B. Compared with the carbonate electrolyte, the decomposition pathway for the ether electrolyte is relatively simple, starting from cleavage of the ether group and forming methane, ethane, ethylene, and organic Li.[182]

In addition to decomposition of the solvent, decomposition of Li salt also generates gas. In the presence of moisture, $LiPF_6$ will hydrolyze to generate HF, which reacts with Li and Al to form LiF and AlF_3 and H_2 gas, Figure 12C. H_2O derived from solvent decomposition can accelerate $LiPF_6$ hydrolysis. The –N-SO_2^- conjunction in LiFSI and LiTFSI will break during decomposition as shown in Figures 12D,E, and then, FSO_2^- fragments in LiFSI will generate SO_2 and F^-.[181,183] In LiTFSI, the $CF_3SO_2^-$ fragment decomposes to CF_3^- and SO_2, and then the trifluoromethyl interacts with H to form CF_3H.[184]

Accumulation of oxygen and flammable gases leads to a significant volume change in cells, especially with pouch cells, leading to poor electrode contact and decreased CE. Electrolyte decomposition is inevitable; a useful strategy is to construct stable CEI/SEI at initial cycling, avoiding further decomposition of electrolytes. Electrochemical mass spectrometry can be used to obtain detailed data regarding gas species and amounts. Differential electrochemical mass spectrometry enables the detection of species in real time, to quantify gas evolution and concurrently determine cell potential and cell current.

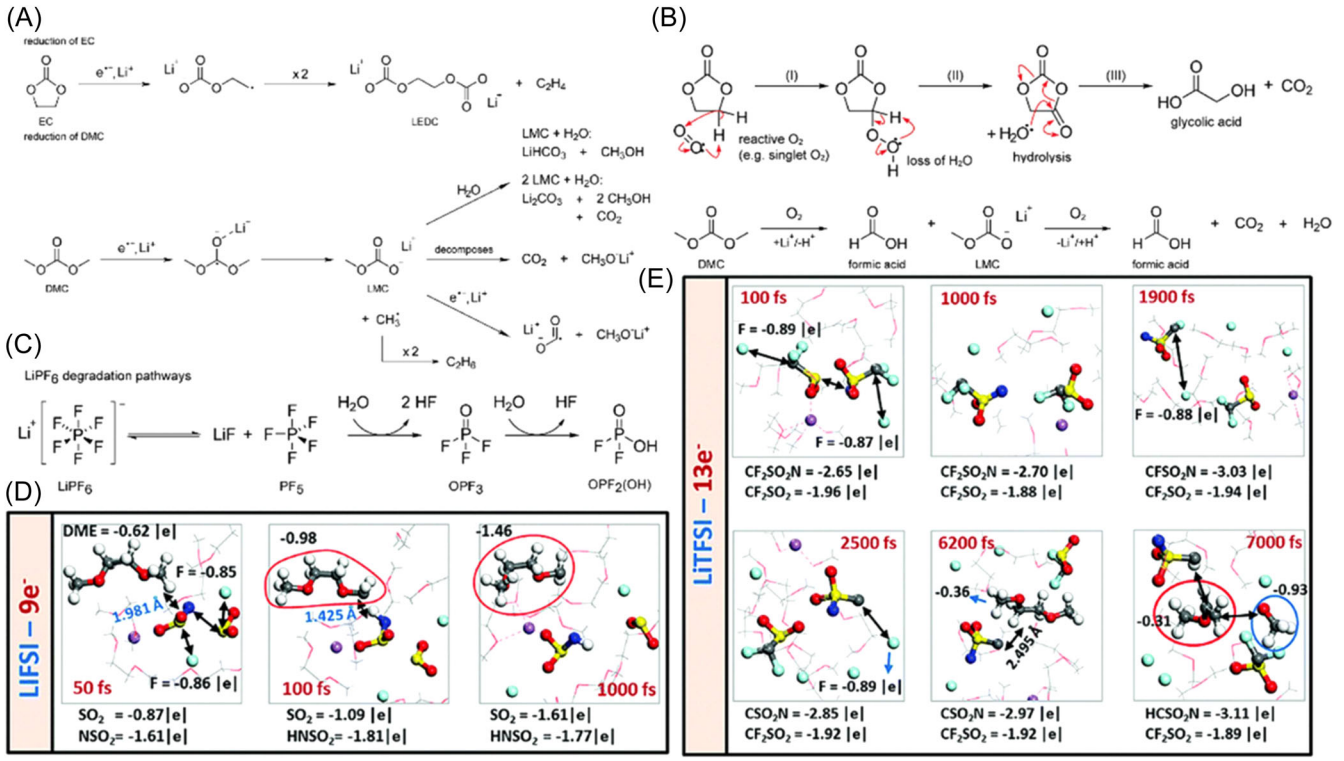

FIGURE 12 (A) Reduction of EC and DMC and (B) mechanism for oxidation of EC and DMC. Reproduced with permission.[180] Copyright 2020, American Chemical Society. (C) $LiPF_6$ decomposition pathways. Reproduced with permission.[180] Copyright 2020, American Chemical Society. (D) LiFSI and (E) LiTFSI reduction using AIMD simulation. Color code: Li = purple; oxygen = red; carbon = gray; fluorine = light blue; sulfur = yellow, nitrogen = blue; and hydrogen = white. Reproduced with permission.[181] Copyright 2017, Royal Society of Chemistry. DMC, dimethyl carbonat; DME, dimethoxyethane; EC, ethylene carbonate.

6.2 | Thermal runaway in LMBs

Internal shorting causes overheating of batteries or thermal runaway. This is a dangerous phenomenon because the flammable carbonate/ether electrolytes will act as fuel, with the oxygen released and the high temperature providing conditions for combustion and explosion.[152,185,186] Therefore, nonflammable solvents and flame-retardant additives are used to improve battery safety.

6.2.1 | Phosphorus-based solvents for safe LMBs

Phosphorus-based solvents, such as TMP and TEP, are the "first" choice for nonflammable electrolytes because the P atoms act as trapping agents for radicals, $H^{\bullet}$ and $OH^{\bullet}$, that are critical for initiating combustion chain reactions, as shown in Figure 13A.[189–194] However, phosphorus-based electrolytes do not generate stable SEI, leading to continuous electrolyte decomposition and poor CE. It is necessary to use additives, such as FEC[195] or $LiNO_3$,[196] to form stable SEI in phosphorus-based electrolytes. Increasing the salt concentration in phosphorus-based electrolyte represents a strategy to improve electrochemical performance, for example, using flame-retardant LiFSI/TMP-based HCE that forms anion-derived SEI and shows stable charge–discharge cycling without additives.[47,187]

6.2.2 | ILs and DES solvents for safe LMBs

ILs and DES solvents with ultrahigh thermal stability and nonflammability are reported as nonflammable electrolytes. A nonflammable 1-ethyl-3-methylimidazolium (EMIm)TFSI electrolyte with sodium bis(trifluoromethanesulfonyl)imide (NaTFSI) as an additive shows 99.6 to 99.9% CE, high discharge voltages up to 4.4 V (vs. Li^+/Li), and high specific capacity, Figure 13B.[93] An SN-based dual-anion deep eutectic solution (D-DES) shows excellent nonflammability and is, therefore, suitable for design of safe electrolytes in LMBs.[172]

6.2.3 | Fluorinated solvent for safe LMBs

Because C–F is more stable than C–H and C–O, fluorination improves thermal stability and nonflammability. In addition,

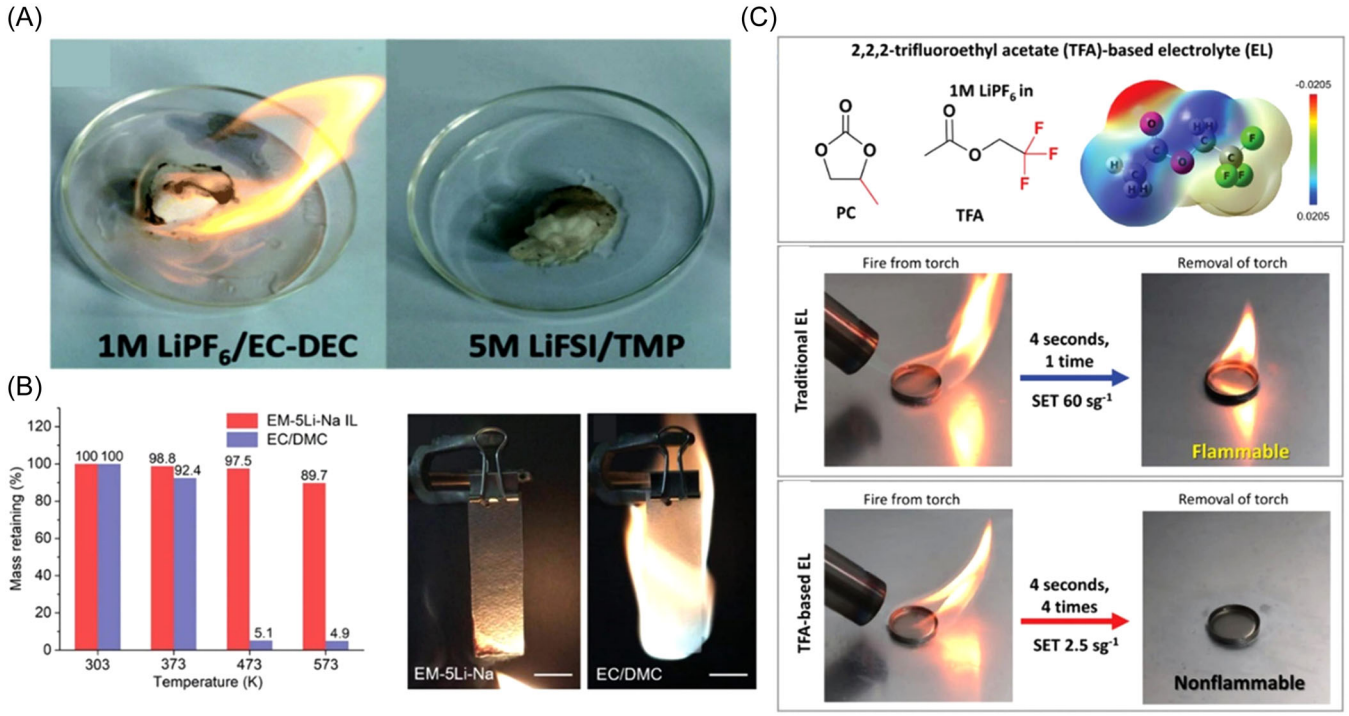

FIGURE 13 (A) Flammability tests for 1 mol/L and TMP-based high-concentration electrolyte. Reproduced with permission.[187] Copyright 2018, Royal Society of Chemistry. (B) Thermal stability and flammability test for ionic liquid and conventional ester electrolyte. Reproduced with permission.[93] Copyright 2020, Wiley-VCH. (C) Chemical structures for the TFA-based electrolyte. Flammability test results for the traditional electrolyte (EL) and TFA-based EL of 1 mol/L $LiPF_6$ in PC/TFA and self-extinguishing time (SET). Reproduced with permission.[188] Copyright 2021, Wiley-VCH. DEC, diethyl carbonate; EC, ethylene carbonate; TMP, trimethyl phosphate.

similar to P atoms, fluorinated solvents generate fluorine radicals (F) that eliminate $H^{\bullet}$ and $OH^{\bullet}$ and terminate the chain reactions induced by harmful free radicals to boost the nonflammability of the electrolytes.[197] Fluorinated cyclic phosphate electrolyte (0.95 mol/L in TFEP) shows excellent nonflammability with zero self-extinguishing time and enables stable cycling of high-voltage $LiNi_{0.5}Mn_{1.5}O_4$ and NCM111 cathodes.[173] Because of the trifluoroethyl group, di-(2,2,2 trifluoroethyl) carbonate shows nonflammability that yields LMBs with improved safety and high operational voltage as shown in Figure 13C. Fire-resistant fluorinated linear ester 2,2,2-trifluoroethyl acetate (TFA) operates under a harsh condition of 4.5 V (vs. Li^+/Li) and shows better performance at 45°C and 2 C.[188,198]

6.2.4 | Fire-retardant additives for safe LMBs

Fire-retardant additives are introduced to reduce the flammability of electrolytes and boost the safety of batteries. Phosphorus-based compounds are also used as fire-retardant additives because of their radical-scavenging ability. Because of the addition of tris(2,2,2-trifluoroethyl) phosphite (TTFP), the EC/DMC-based electrolyte becomes nonflammable.[199] 2-ethoxy-2,4,4,6,6-pentafluoro-1,3,5,2,4,6-triazatriphosphorine is also used as an additive in carbonate electrolytes to retard ignition.[200] Nanoparticles are also used as fire-retardant additives including LiF nanobox.[74] Because nonflammable solvents as electrolytes cannot produce stable SEI to show better cycling stability, use of fire-retardant additives in traditional electrolytes to balance cycling stability and safety is the best choice.

7 | LOW-COST ELECTROLYTES IN LMBs

Cost is a significant design factor in the large-scale application of LMBs. Although IL electrolytes show high-temperature performance, nonflammability, and high stability against oxidation, their high-cost limits practical large-scale applications. DES is a better cost choice. A drawback, however, is that the electrochemical performance of DES electrolytes needs to be improved. Fluorinated ether electrolytes improve stability against oxidation and modulate the Li^+ solvation environment to show better cycling performance. However, a complex synthesis and purification increases the cost. HCEs have

been reportedly successful at high voltage, a wide range of temperatures, high cycling stability, and fast charging. A drawback is that the need for high concentrations of Li salt increases the cost. In LHCEs, hydrofluoroethers that are volatile and insoluble in water are released into the environment, contributing to global warming.[201] Because of stable C–F bonds, fluorinated compounds are practically difficult to decompose and will contaminate the local environment. Compared with improved solvents, use of additives represents a better method because of the need for a smaller number of additives to induce improved performance. It appears, therefore, that it is more economical to boost battery performance via incremental design incorporation of components in the electrolyte and not replacing the skeletal composition. This is evidenced by the fact that the reported research has focused on additives and not developments in solvents and Li salts.

8 | CONCLUSIONS AND PERSPECTIVES

Next-generation LMBs with higher energy density will evolve for long lifespan, wide range of working temperatures, and fast charge for boosted energy storage. Targeted electrolyte design will play a vital role in achieving high-performance LMBs by eliminating Li dendrites and achieving stable Li plating/stripping. Evolution will be highly dependent on an improved understanding of the fundamental mechanisms of electrolyte in different working conditions. Importantly, high ion conductivity together with facile de-solvation is a practical prerequisite for LMBs with fast charge and low working temperature. De-solvation energy is linked to the solvent used; weakening the solvated interaction between Li^+ and solvent molecules can lead to lower de-solvated barriers. Current methods include use of weakly solvated solvents and fluorinated ether electrolytes. HCEs and LHCEs also show facile de-solvation for fast charge and working at low temperatures, because abound CIPs and AGGs result in lower de-solvation energy. For high working temperatures and high anodic voltages, together with increased safety, the electrolyte should have high thermal and high electrochemical stability. Because it is practically difficult to synthesize an electrolyte with a single solvent or a single salt to meet all the requirements for high-performance of LMBs, co-solvents and additives can be used to balance ion conductivity, anodic stability, thermal stability, and solvated environment.

For continued evolution of high-performance LMBs, it is important to form a stable SEI. SEI consists of organic and inorganic compounds. Organic compounds may dissolve in the electrolyte and result in poor passivation ability; inorganic compounds including LiF and Li_2O with high interfacial energy can passivate the Li anode to show stable Li deposition. Because of this, the present design methods focus on the generation of inorganic-enriched SEI. However, SEI with reduced organic compounds shows higher Young's modulus, and is fragile and not able to form a homogeneous film on the anode.

More detailed knowledge of SEI is necessary for continued development of Li anodes. In situ advanced characterization techniques will be needed to capture the real-time dynamics of SEI and will include transmission electron microscopy, atomic force microscopy, X-ray photoelectron spectroscopy, electron paramagnetic resonance, and nuclear magnetic resonance (NMR).

HCE, LHCE, and fluorinated ether electrolyte form stable anion-derived SEI and boost electrochemical performance by modifying the Li^+ solvation environment and generating sufficient AGGs and CIPs. The Li^+ solvation environment is therefore very important in the formation of stable SEI in LMBs. Current technologies to characterize solvation shells include Raman and NMR. In Raman, information is obtained through characteristic vibrational peaks for the anion. With NMR, which is more sensitive to the coordination species in the solvation shell, the upfield or downfield shift indicates an increase or decrease in electron density around Li^+.

Use of a solid-state electrolyte is a practical alternative solution for high-performance LMBs. A carefully designed solid-state electrolyte with significant value for Young's modulus will eliminated Li dendrites to result in stable cycling. Polymer-based solid-sate electrolytes are more advantageous in flexible devices. However, Li dendrite growth at grain boundaries can occur because of the high electronic conductivity of inorganic solid-state electrolyte and reduce the electrochemical performance of solid-state batteries. The high contact resistance in inorganic solid-state electrolytes and the low ion conductivity at RT in polymer-based solid-state electrolytes can lead to poor electrochemical performance and lower energy density. Therefore, more research is needed in both liquid and solid-state electrolytes.

Although the “ideal” electrolyte is water as an environmentally benign solvent, protic solvents are not compatible with Li anodes and therefore hinder practical application. Chemical wastes from the preparation of electrodes and waste electrode materials and electrolytes could pose a threat to a sustainable environment. Therefore, future research needs to be focused on designs to improve the environmentally friendly nature of LMBs.

LMBs are a complex system. Based on a "wood barrel" principle, it is necessary to identify and solve "short board," for example, cathode, anode, electrolyte, and separator, to evolve to advanced forms. We firmly believe that the large application of LMBs will be successful with the continuous efforts of researchers.

ACKNOWLEDGMENTS

Financial support provided by the Australian Research Council (ARC) (FL210100050, LP160101629, and DP210101486) is gratefully acknowledged. Mingnan Li acknowledges the Chinese Sponsorship Council for scholarship support (No. 202106130006).

CONFLICTS OF INTEREST STATEMENT

The authors declare no conflicts of interest.

ORCID

Zaiping Guo http://orcid.org/0000-0003-3464-5301

REFERENCES

1. Tarascon JM, Armand M. Issues and challenges facing rechargeable lithium batteries. *Nature*. 2001;414(6861):359-367.
2. Wu J, Cao Y, Zhao H, Mao J, Guo Z. The critical role of carbon in marrying silicon and graphite anodes for high-energy lithium-ion batteries. *Carbon Energy*. 2019;1(1):57-76.
3. Liang G, Wu Z, Didier C, et al. A long cycle-life high-voltage spinel lithium-ion battery electrode achieved by site-selective doping. *Angew Chem Int Ed*. 2020;59(26):10594-10602.
4. Hu S, Pillai AS, Liang G, et al. Li-rich layered oxides and their practical challenges: recent progress and perspectives. *Electrochem Energy Rev*. 2019;2(2):277-311.
5. High energy lithium batteries for electric vehicles. Accessed January 1, 2023. https://www.energy.gov/sites/default/files/2019/06/f64/bat247_lopez_2019_p_6.3_4.48pm_jl.pdf
6. Yang XG, Liu T, Wang CY. Thermally modulated lithium iron phosphate batteries for mass-market electric vehicles. *Nat Energy*. 2021;6(2):176-185.
7. Zhou J, Zhang S, Zhou YN, et al. Biomass-derived carbon materials for high-performance supercapacitors: current status and perspective. *Electrochem Energy Rev*. 2021;4(2):219-248.
8. Wang J, Wang Z, Ni J, Li L. Electrospun materials for batteries moving beyond lithium-ion technologies. *Electrochem Energy Rev*. 2022;5(2):211-241.
9. Zhang S, Liu Y, Fan Q, et al. Liquid metal batteries for future energy storage. *Energy Environ Sci*. 2021;14(8):4177-4202.
10. Zhang S, Sun L, Fan Q, et al. Challenges and prospects of lithium–CO_2 batteries. *Nano Res*. 2022;1(1):e9120001.
11. Extreme fast charge lithium ion batteries. Accessed January 1, 2023. https://www.energy.gov/sites/default/files/2020/06/f75/bat398_buiel_2020_o_5.20.20_456PM_LR.pdf
12. Winslow KM, Laux SJ, Townsend TG. A review on the growing concern and potential management strategies of waste lithium-ion batteries. *Resour Conserv Recy*. 2018;129:263-277.
13. Ziemann S, Müller DB, Schebek L, Weil M. Modeling the potential impact of lithium recycling from EV batteries on lithium demand: a dynamic MFA approach. *Resour Conserv Recy*. 2018;133:76-85.
14. Zhang SS. Challenges and strategies for fast charge of Li-ion batteries. *ChemElectroChem*. 2020;7(17):3569-3577.
15. Zhu GL, Zhao CZ, Huang JQ, et al. Fast charging lithium batteries: recent progress and future prospects. *Small*. 2019;15(15):1805389.
16. Wang X, Salari M, Jiang D, et al. Electrode material-ionic liquid coupling for electrochemical energy storage. *Nat Rev Mater*. 2020;5(11):787-808.
17. Feng Y, Zhou L, Ma H, et al. Challenges and advances in wide-temperature rechargeable lithium batteries. *Energy Environ Sci*. 2022;15(5):1711-1759.
18. Zhang N, Deng T, Zhang S, et al. Critical review on low-temperature Li-ion/metal batteries. *Adv Mater*. 2022;34(15):2107899.
19. Ma S, Jiang M, Tao P, et al. Temperature effect and thermal impact in lithium-ion batteries: a review. *Prog Nat Sci Mater Inter*. 2018;28(6):653-666.
20. Jie Y, Ren X, Cao R, Cai W, Jiao S. Advanced liquid electrolytes for rechargeable Li metal batteries. *Adv Funct Mater*. 2020;30(25):1910777.
21. Winter M, Barnett B, Xu K. Before Li ion batteries. *Chem Rev*. 2018;118(23):11433-11456.
22. Lin D, Liu Y, Cui Y. Reviving the lithium metal anode for high-energy batteries. *Nat Nanotechnol*. 2017;12(3):194-206.
23. Xiao J. How lithium dendrites form in liquid batteries. *Science*. 2019;366(6464):426-427.
24. Feng X, Wu HH, Gao B, Świętosławski M, He X, Zhang Q. Lithiophilic N-doped carbon bowls induced Li deposition in layered graphene film for advanced lithium metal batteries. *Nano Res*. 2022;15(1):352-360.
25. Liu B, Zhang J-G, Xu W. Advancing lithium metal batteries. *Joule*. 2018;2(5):833-845.
26. Xu K. Nonaqueous liquid electrolytes for lithium-based rechargeable batteries. *Chem Rev*. 2004;104(10):4303-4418.
27. Wang Z, Wang Y, Zhang Z, et al. Building artificial solid-electrolyte interphase with uniform intermolecular ionic bonds toward dendrite-free lithium metal anodes. *Adv Funct Mater*. 2020;30(30):2002414.
28. Wang Y, Wang Z, Zhao L, et al. Lithium metal electrode with increased air stability and robust solid electrolyte interphase realized by silane coupling agent modification. *Adv Mater*. 2021;33(14):2008133.
29. Wang Z, Wang Y, Wu C, Pang WK, Mao J, Guo Z. Constructing nitrided interfaces for stabilizing Li metal electrodes in liquid electrolytes. *Chem Sci*. 2021;12(26):8945-8966.
30. Liang H, Wang L, Sheng L, Xu H, Song Y, He X. Focus on the electroplating chemistry of Li ions in nonaqueous liquid electrolytes: toward stable lithium metal batteries. *Electrochem Energy Rev*. 2022;5(2):23.
31. Chen Y, Yu Z, Rudnicki P, et al. Steric effect tuned ion solvation enabling stable cycling of high-voltage lithium metal battery. *J Am Chem Soc*. 2021;143(44):18703-18713.
32. Yu Z, Rudnicki PE, Zhang Z, et al. Rational solvent molecule tuning for high-performance lithium metal battery electrolytes. *Nat Energy*. 2022;7(1):94-106.

33. Hobold GM, Lopez J, Guo R, et al. Moving beyond 99.9% Coulombic efficiency for lithium anodes in liquid electrolytes. *Nat Energy*. 2021;6(10):951-960.
34. Wang Y, Wang Z, Yang F, et al. Electrolyte engineering enables high performance zinc-ion batteries. *Small*. 2022;18(43):2107033.
35. Mao J, Wang C, Lyu Y, et al. Organic electrolyte design for practical potassium-ion batteries. *J Mater Chem A*. 2022;10(37):19090-19106.
36. Fan X, Ji X, Chen L, et al. All-temperature batteries enabled by fluorinated electrolytes with non-polar solvents. *Nat Energy*. 2019;4(10):882-890.
37. Holoubek J, Liu H, Wu Z, et al. Tailoring electrolyte solvation for Li metal batteries cycled at ultra-low temperature. *Nat Energy*. 2021;6(3):303-313.
38. Zheng J, Engelhard MH, Mei D, et al. Electrolyte additive enabled fast charging and stable cycling lithium metal batteries. *Nat Energy*. 2017;2(3):17012.
39. Yamada Y, Furukawa K, Sodeyama K, et al. Unusual stability of acetonitrile-based superconcentrated electrolytes for fast-charging lithium-ion batteries. *J Am Chem Soc*. 2014;136(13):5039-5046.
40. Zheng ZJ, Ye H, Guo ZP. Recent progress in designing stable composite lithium anodes with improved wettability. *Adv Sci*. 2020;7(22):2002212.
41. Yamada Y, Wang J, Ko S, Watanabe E, Yamada A. Advances and issues in developing salt-concentrated battery electrolytes. *Nat Energy*. 2019;4(4):269-280.
42. Xiao Y, Xu R, Xu L, Ding J-F, Huang J-Q. Recent advances in anion-derived SEIs for fast-charging and stable lithium batteries. *Energy Mater*. 2021;1:100013.
43. Ren F, Li Z, Chen J, Huguet P, Peng Z, Deabate S. Solvent-diluent interaction-mediated solvation structure of localized high-concentration electrolytes. *ACS Appl Mater Interfaces*. 2022;14(3):4211-4219.
44. Chen X, Yao N, Zeng B-S, Zhang Q. Ion–solvent chemistry in lithium battery electrolytes: from mono-solvent to multi-solvent complexes. *Fundam Res*. 2021;1(4):393-398.
45. Yamada Y, Yamada A. Superconcentrated electrolytes for lithium batteries. *J Electrochem Soc*. 2015;162(14):A2406.
46. Qian J, Henderson WA, Xu W, et al. High rate and stable cycling of lithium metal anode. *Nat Commun*. 2015;6(1):6362.
47. Wang J, Yamada Y, Sodeyama K, et al. Fire-extinguishing organic electrolytes for safe batteries. *Nat Energy*. 2018;3(1):22-29.
48. Wang J, Yamada Y, Sodeyama K, Chiang CH, Tateyama Y, Yamada A. Superconcentrated electrolytes for a high-voltage lithium-ion battery. *Nat Commun*. 2016;7(1):12032.
49. Alvarado J, Schroeder MA, Zhang M, et al. A carbonate-free, sulfone-based electrolyte for high-voltage Li-ion batteries. *Mater Today*. 2018;21(4):341-353.
50. Jiao S, Ren X, Cao R, et al. Stable cycling of high-voltage lithium metal batteries in ether electrolytes. *Nat Energy*. 2018;3(9):739-746.
51. Louli AJ, Eldesoky A, Weber R, et al. Diagnosing and correcting anode-free cell failure via electrolyte and morphological analysis. *Nat Energy*. 2020;5(9):693-702.
52. Pham TD, Bin Faheem A, Lee KK. Design of a LiF-rich solid electrolyte interphase layer through highly concentrated LiFSI–THF electrolyte for stable lithium metal batteries. *Small*. 2021;17(46):2103375.
53. Suo L, Xue W, Gobet M, et al. Fluorine-donating electrolytes enable highly reversible 5-V-class Li metal batteries. *Proc Natl Acad Sci USA*. 2018;115(6):1156-1161.
54. Chen S, Zheng J, Mei D, et al. High-voltage lithium-metal batteries enabled by localized high-concentration electrolytes. *Adv Mater*. 2018;30(21):1706102.
55. Wang H, Matsui M, Kuwata H, et al. A reversible dendrite-free high-areal-capacity lithium metal electrode. *Nat Commun*. 2017;8(1):15106.
56. Ueno K, Murai J, Moon H, Dokko K, Watanabe M. A design approach to lithium-ion battery electrolyte based on diluted solvate ionic liquids. *J Electrochem Soc*. 2017;164(1):A6088-A6094.
57. Peng X, Lin Y, Wang Y, Li Y, Zhao T. A lightweight localized high-concentration ether electrolyte for high-voltage Li-ion and Li-metal batteries. *Nano Energy*. 2022;96:107102.
58. Fan X, Chen L, Borodin O, et al. Author correction: non-flammable electrolyte enables Li-metal batteries with aggressive cathode chemistries. *Nat Nanotechnol*. 2018;13(12):1191.
59. Zheng Y, Soto FA, Ponce V, et al. Localized high concentration electrolyte behavior near a lithium-metal anode surface. *J Mater Chem A*. 2019;7(43):25047-25055.
60. Jiang LL, Yan C, Yao YX, Cai W, Huang JQ, Zhang Q. Inhibiting solvent co-intercalation in a graphite anode by a localized high-concentration electrolyte in fast-charging batteries. *Angew Chem Int Ed*. 2021;60(7):3402-3406.
61. Zhao Y, Zhou T, Ashirov T, et al. Fluorinated ether electrolyte with controlled solvation structure for high voltage lithium metal batteries. *Nat Commun*. 2022;13(1):2575.
62. Yu Z, Wang H, Kong X, et al. Molecular design for electrolyte solvents enabling energy-dense and long-cycling lithium metal batteries. *Nat Energy*. 2020;5(7):526-533.
63. Ichino T, Sasaki S, Matsuura T, Nishi S. Synthesis and properties of new polyimides containing flourinated alkoxy side chains. *J Polym Sci Part A Polym Chem*. 1990;28(2):323-331.
64. Fu J, Ji X, Chen J, et al. Lithium nitrate regulated sulfone electrolytes for lithium metal batteries. *Angew Chem Int Ed*. 2020;59(49):22194-22201.
65. Xu R, Shen X, Ma XX, et al. Identifying the critical anion-cation coordination to regulate the electric double layer for an efficient lithium-metal anode interface. *Angew Chem Int Ed*. 2021;60(8):4215-4220.
66. Yan C, Li HR, Chen X, et al. Regulating the inner Helmholtz plane for stable solid electrolyte interphase on lithium metal anodes. *J Am Chem Soc*. 2019;141(23):9422-9429.
67. Wang X, Wang S, Wang H, et al. Hybrid electrolyte with dual-anion-aggregated solvation sheath for stabilizing high-voltage lithium-metal batteries. *Adv Mater*. 2021;33(52):2007945.
68. Wang ZJ, Wang YY, Li BH, et al. Non-flammable ester electrolyte with boosted stability against Li for high-performance Li metal batteries. *Angew Chem Int Edit*. 2022;61:e2022066.
69. Zhang R, Cheng XB, Zhao CZ, et al. Conductive nanostructured scaffolds render low local current density to inhibit lithium dendrite growth. *Adv Mater*. 2016;28(11):2155-2162.
70. Zhu Y, He S, Ding J, Zhao G, Lian F. The sulfolane-based liquid electrolyte with $LiClO_4$ additive for the wide-temperature

operating high nickel ternary cathode. *Nano Res.* 2022;12274: 1-9. doi:10.1007/s12274-022-4852-y

71. Lee SH, Hwang JY, Ming J, et al. Toward the sustainable lithium metal batteries with a new electrolyte solvation chemistry. *Adv Energy Mater.* 2020;10(20):2000567.
72. Li T, Zhang XQ, Yao N, et al. Stable anion-derived solid electrolyte interphase in lithium metal batteries. *Angew Chem.* 2021;133(42):22865-22869.
73. Kim MS, Zhang Z, Rudnicki PE, et al. Suspension electrolyte with modified Li+ solvation environment for lithium metal batteries. *Nat Mater.* 2022;21(4):445-454.
74. Tan YH, Lu GX, Zheng JH, et al. Lithium fluoride in electrolyte for stable and safe lithium-metal batteries. *Adv Mater.* 2021;33(42):2102134.
75. Shen L, Wu HB, Liu F, et al. Particulate anion sorbents as electrolyte additives for lithium batteries. *Adv Funct Mater.* 2020;30(49):2003055.
76. Yu Y, Zhang X-B. In situ coupling of colloidal silica and Li salt anion toward stable Li anode for long-cycle-life Li-O_2. *Matter.* 2019;1(4):881-892.
77. Li T, Zhang XQ, Shi P, Zhang Q. Fluorinated solid-electrolyte interphase in high-voltage lithium metal batteries. *Joule.* 2019;3(11):2647-2661.
78. Zhang XQ, Cheng XB, Chen X, Yan C, Zhang Q. Fluoroethylene carbonate additives to render uniform Li deposits in lithium metal batteries. *Adv Funct Mater.* 2017;27(10):1605989.
79. Piao N, Liu S, Zhang B, et al. Lithium metal batteries enabled by synergetic additives in commercial carbonate electrolytes. *ACS Energy Lett.* 2021;6(5):1839-1848.
80. Seng KH, Li L, Chen DP, et al. The effects of FEC (fluoroethylene carbonate) electrolyte additive on the lithium storage properties of NiO (nickel oxide) nanocuboids. *Energy.* 2013;58(1):707-713.
81. Zhao W, Ren F, Yan Q, Liu H, Yang Y. A facile synthesis of non-aqueous $LiPO_2F_2$ solution as the electrolyte additive for high performance lithium ion batteries. *Chin Chem Lett.* 2020;31(12):3209-3212.
82. Chen Y, Zhao W, Zhang Q, et al. Armoring $LiNi_{1/3}Co_{1/3}Mn_{1/3}O_2$ cathode with reliable fluorinated organic–inorganic hybrid interphase layer toward durable high rate battery. *Adv Funct Mater.* 2020;30(19):2000396.
83. Mosallanejad B, Sadeghi Malek S, Ershadi M, et al. Insights into the efficient roles of solid electrolyte interphase derived from vinylene carbonate additive in rechargeable batteries. *J Electroanal Chem.* 2022;909:116126.
84. Wu H, Tang B, Du X, et al. LiDFOB initiated in situ polymerization of novel eutectic solution enables room-temperature solid lithium metal batteries. *Adv Sci.* 2020;7(23):2003370.
85. Xu K, Zhang S, Jow TR, Xu W, Angell CA. LiBOB as salt for lithium-ion batteries: a possible solution for high temperature operation. *Electrochem Solid-State Lett.* 2002;5(1):A26-A29.
86. Yu J, Liu J, Lin X, et al. A solid-like dual-salt polymer electrolyte for Li-metal batteries capable of stable operation over an extended temperature range. *Energy Storage Mater.* 2021;37:609-618.
87. Zhang H, Eshetu GG, Judez X, Li C, Rodriguez-Martínez LM, Armand M. Electrolyte additives for lithium metal anodes and rechargeable lithium metal batteries: progress and perspectives. *Angew Chem Int Ed.* 2018;57(46): 15002-15027.
88. Zhai P, Liu L, Gu X, Wang T, Gong Y. Interface engineering for lithium metal anodes in liquid electrolyte. *Adv Energy Mater.* 2020;10(34):2001257.
89. Qin K, Holguin K, Mohammadiroudbari M, et al. Strategies in structure and electrolyte design for high-performance lithium metal batteries. *Adv Funct Mater.* 2021;31(15): 2009694.
90. Ren X, Chen S, Lee H, et al. Localized high-concentration sulfone electrolytes for high-efficiency lithium-metal batteries. *Chem.* 2018;4(8):1877-1892.
91. Wen Z, Fang W, Wu X, et al. High-concentration additive and triiodide/iodide redox couple stabilize lithium metal anode and rejuvenate the inactive lithium in carbonate-based electrolyte. *Adv Funct Mater.* 2022;32:2204768.
92. Yang Y, Davies DM, Yin Y, et al. High-efficiency lithium-metal anode enabled by liquefied gas electrolytes. *Joule.* 2019;3(8):1986-2000.
93. Sun H, Zhu G, Zhu Y, et al. High-safety and high-energy-density lithium metal batteries in a novel ionic-liquid electrolyte. *Adv Mater.* 2020;32(26):2001741.
94. Ma T, Xu GL, Li Y, et al. Revisiting the corrosion of the aluminum current collector in lithium-ion batteries. *J Phys Chem Lett.* 2017;8(5):1072-1077.
95. Morita M, Shibata T, Yoshimoto N, Ishikawa M. Anodic behavior of aluminum in organic solutions with different electrolytic salts for lithium ion batteries. *Electrochim Acta.* 2002;47(17):2787-2793.
96. Li L, Fu L, Li M, et al. B-doped and La_4NiLiO_8-coated Ni-rich cathode with enhanced structural and interfacial stability for lithium-ion batteries. *J Energy Chem.* 2022;71:588-594.
97. Yang H, Kwon K, Devine TM, Evans JW. Aluminum corrosion in lithium batteries - an investigation using the electrochemical quartz crystal microbalance. *J Electrochem Soc.* 2000;147(12):4399-4407.
98. Zhou Q, Fu C, Li R, et al. Poly (vinyl ethylene carbonate)-based dual-salt gel polymer electrolyte enabling high voltage lithium metal batteries. *Chem Eng J.* 2022;437:135419.
99. Geng Z, Huang Y, Sun G, et al. In-situ polymerized solid-state electrolytes with stable cycling for Li/LiCoO2 batteries. *Nano Energy.* 2022;91:106679.
100. Boyle DT, Huang W, Wang H, et al. Corrosion of lithium metal anodes during calendar ageing and its microscopic origins. *Nat Energy.* 2021;6(5):487-494.
101. Qiao L, Oteo U, Martinez-Ibañez M, et al. Stable non-corrosive sulfonimide salt for 4-V-class lithium metal batteries. *Nat Mater.* 2022;21(4):455-462.
102. Zhang Z, Wang X, Bai Y, Wu C. Charactering and optimizing cathode electrolytes interface for advanced rechargeable batteries: promises and challenges. *Green Energy Environ.* 2022;7(4):606-635.
103. Sun Z, Li M, Xiao B, et al. In situ transmission electron microscopy for understanding materials and interfaces challenges in all-solid-state lithium batteries. *Etransportation.* 2022;14:100203.
104. Wang C, Tan L, Yi H, et al. Unveiling the impact of residual Li conversion and cation ordering on electrochemical

performance of Co-free Ni-rich cathodes. *Nano Res*. 2022;15(10):9038-9046.
105. Jiao S, Zheng J, Li Q, et al. Behavior of lithium metal anodes under various capacity utilization and high current density in lithium metal batteries. *Joule*. 2018;2(1):110-124.
106. Deng T, Fan X, Cao L, et al. Designing in-situ-formed interphases enables highly reversible cobalt-free $LiNiO_2$ cathode for Li-ion and Li-metal batteries. *Joule*. 2019;3(10):2550-2564.
107. Han JG, Park I, Cha J, et al. Interfacial architectures derived by lithium difluoro(bisoxalato) phosphate for lithium-rich cathodes with superior cycling stability and rate capability. *ChemElectroChem*. 2017;4(1):56-65.
108. Jiang B, Li J, Luo B, et al. $LiPO_2F_2$ electrolyte additive for high-performance Li-rich cathode material. *J Energy Chem*. 2021;60:564-571.
109. Zhang W, Yang T, Zhao K, Liao X, Zhao Y. Accurate redox potentials for solvents in Li-metal batteries and assessment of density functionals. *Int J Quantum Chem*. 2022;122(10):e26886.
110. El Ouatani L, Dedryvère R, Siret C, et al. The effect of vinylene carbonate additive on surface film formation on both electrodes in Li-ion batteries. *J Electrochem Soc*. 2009;156(2):A103-A113.
111. Qian Y, Niehoff P, Börner M, et al. Influence of electrolyte additives on the cathode electrolyte interphase (CEI) formation on $LiNi_{1/3}Mn_{1/3}Co_{1/3}O_2$ in half cells with Li metal counter electrode. *J Power Sources*. 2016;329:31-40.
112. Zou L, Gao P, Jia H, et al. Nonsacrificial additive for tuning the cathode-electrolyte interphase of lithium-ion batteries. *ACS Appl Mater Interfaces*. 2022;14(3):4111-4118.
113. Hekmatfar M, Hasa I, Eghbal R, Carvalho DV, Moretti A, Passerini S. Effect of electrolyte additives on the $LiNi_{0.5}Mn_{0.3}Co_{0.2}O_2$ surface film formation with lithium and graphite negative electrodes. *Adv Mater Interfaces*. 2020;7(1):1901500.
114. Li M, Zhang J, Gao Y, Wang X, Zhang Y, Zhang S. A water-soluble, adhesive and 3D cross-linked polyelectrolyte binder for high-performance lithium-sulfur batteries. *J Mater Chem A*. 2021;9(4):2375-2384.
115. Li M, Liu Z, Zhang Y, Wang X, Zhang C, Zhang S. Nitrogen-doped microporous carbon with narrow pore size distribution as sulfur host to encapsulate small sulfur molecules for highly stable lithium-sulfur batteries. *J Solid State Electrochem*. 2021;25(4):1293-1302.
116. Wang H, Zhang W, Xu J, Guo Z. Advances in polar materials for lithium-sulfur batteries. *Adv Funct Mater*. 2018;28(38):1707520.
117. Zheng ZJ, Ye H, Guo ZP. Recent progress on pristine metal/covalent-organic frameworks and their composites for lithium-sulfur batteries. *Energy Environ Sci*. 2021;14(4):1835-1853.
118. Suo L, Hu YS, Li H, Armand M, Chen L. A new class of Solvent-in-Salt electrolyte for high-energy rechargeable metallic lithium batteries. *Nat Commun*. 2013;4(1):1481.
119. Cuisinier M, Cabelguen PE, Adams BD, Garsuch A, Balasubramanian M, Nazar LF. Unique behaviour of nonsolvents for polysulphides in lithium-sulphur batteries. *Energy Environ Sci*. 2014;7(8):2697-2705.
120. Wang X, Tan Y, Shen G, Zhang S. Recent progress in fluorinated electrolytes for improving the performance of Li-S batteries. *J Energy Chem*. 2020;41:149-170.
121. Azimi N, Xue Z, Bloom I, et al. Understanding the effect of a fluorinated ether on the performance of lithium-sulfur batteries. *ACS Appl Mater Interfaces*. 2015;7(17):9169-9177.
122. Dokko K, Tachikawa N, Yamauchi K, et al. Solvate ionic liquid electrolyte for Li-S batteries. *J Electrochem Soc*. 2013;160(8):A1304-A1310.
123. Wang L, Liu J, Yuan S, Wang Y, Xia Y. To mitigate self-discharge of lithium-sulfur batteries by optimizing ionic liquid electrolytes. *Energy Environ Sci*. 2016;9(1):224-231.
124. Liu T, Li H, Yue J, et al. Ultralight electrolyte for high-energy lithium-sulfur pouch cells. *Angew Chem Int Ed*. 2021;60(32):17547-17555.
125. Cheng Q, Xu W, Qin S, et al. Full dissolution of the whole lithium sulfide family (Li_2S_8 to Li_2S) in a safe eutectic solvent for rechargeable lithium-sulfur batteries. *Angew Chem Int Ed*. 2019;58(17):5557-5561.
126. Pan H, Chen J, Cao R, et al. Non-encapsulation approach for high-performance Li–S batteries through controlled nucleation and growth. *Nat Energy*. 2017;2(10):813-820.
127. Fan Q, Jiang J, Zhang S, et al. Accelerated polysulfide redox in binder-free Li_2S cathodes promises high-energy-density lithium-sulfur batteries. *Adv Energy Mater*. 2021;11(32):2100957.
128. Jangir AK, Sethy P, Verma G, Bahadur P, Kuperkar K. An inclusive thermophysical and rheology portrayal of deep eutectic solvents (DES) for metal oxides dissolution enhancement. *J Mol Liq*. 2021;332:115909.
129. Wu F, Chu F, Ferrero GA, et al. Boosting high-performance in lithium-sulfur batteries via dilute electrolyte. *Nano Lett*. 2020;20(7):5391-5399.
130. Nakanishi A, Ueno K, Watanabe D, et al. Sulfolane-based highly concentrated electrolytes of lithium bis(trifluoromethanesulfonyl)amide: ionic transport, Li-ion coordination, and Li-S battery performance. *J Phys Chem C*. 2019;123(23):14229-14238.
131. Liu Y, Zhu Y, Cui Y. Challenges and opportunities towards fast-charging battery materials. *Nat Energy*. 2019;4(7):540-550.
132. Narita A, Shibayama W, Sakamoto K, Mizumo T, Matsumi N, Ohno H. Lithium ion conduction in an organoborate zwitterion-LiTFSI mixture. *Chem Commun*. 2006;18(1):1926-1928.
133. Makhlooghiazad F, O'Dell LA, Porcarelli L, et al. Zwitterionic materials with disorder and plasticity and their application as non-volatile solid or liquid electrolytes. *Nat Mater*. 2022;21(2):228-236.
134. Kim D, Liu X, Yu B, et al. Amine-functionalized boron nitride nanosheets: a new functional additive for robust, flexible ion gel electrolyte with high lithium-ion transference number. *Adv Funct Mater*. 2020;30(15):1910813.
135. Cho SK, Oh KS, Shin JC, et al. Anion-rectifying polymeric single lithium-ion conductors. *Adv Funct Mater*. 2022;32(6):2107753.
136. Wen B, Deng Z, Tsai PC, et al. Ultrafast ion transport at a cathode-electrolyte interface and its strong dependence on salt solvation. *Nat Energy*. 2020;5(8):578-586.
137. Gupta A, Manthiram A. Designing advanced lithium-based batteries for low-temperature conditions. *Adv Energy Mater*. 2020;10(38):2001972.
138. Liu S, Zhang R, Mao J, Zhao Y, Cai Q, Guo Z. From room temperature to harsh temperature applications:

fundamentals and perspectives on electrolytes in zinc metal batteries. *Sci Adv*. 2022;8(12):eabn5097.
139. Li Q, Liu G, Cheng H, Sun Q, Zhang J, Ming J. Low-temperature electrolyte design for lithium-ion batteries: prospect and challenges. *Chem Euro J*. 2021;27(64):15842-15865.
140. Rustomji CS, Yang Y, Kim TK, et al. Liquefied gas electrolytes for electrochemical energy storage devices. *Science*. 2017;356(6345):1351.
141. Yang Y, Yin Y, Davies DM, et al. Liquefied gas electrolytes for wide-temperature lithium metal batteries. *Energy Environ Sci*. 2020;13(7):2209-2219.
142. Yin Y, Yang Y, Cheng D, et al. Fire-extinguishing, recyclable liquefied gas electrolytes for temperature-resilient lithium-metal batteries. *Nat Energy*. 2022;7(6):548-559.
143. Thenuwara AC, Shetty PP, McDowell MT. Distinct nanoscale interphases and morphology of lithium metal electrodes operating at low temperatures. *Nano Lett*. 2019;19(12):8664-8672.
144. Ma T, Ni YX, Wang QR, et al. Optimize lithium deposition at low temperature by weakly solvating power solvent. *Angew Chem Int Edit*. 2022;134:e202207.
145. Wang J, Huang W, Pei A, et al. Improving cyclability of Li metal batteries at elevated temperatures and its origin revealed by cryo-electron microscopy. *Nat Energy*. 2019;4(8):664-670.
146. Ko S, Obukata T, Shimada T, et al. Electrode potential influences the reversibility of lithium-metal anodes. *Nat Energy*. 2022;7(1):1217-1224.
147. Lin S, Hua H, Lai P, Zhao J. A multifunctional dual-salt localized high-concentration electrolyte for fast dynamic high-voltage lithium battery in wide temperature range. *Adv Energy Mater*. 2021;11(36):2101775.
148. Lin X, Kavian R, Lu Y, Hu Q, Shao-Horn Y, Grinstaff MW. Thermally-responsive, nonflammable phosphonium ionic liquid electrolytes for lithium metal batteries: operating at 100 degrees celsius. *Chem Sci*. 2015;6(11):6601-6606.
149. Jaumaux P, Liu Q, Zhou D, et al. Deep-eutectic-solvent-based self-healing polymer electrolyte for safe and long-life lithium-metal batteries. *Angew Chem Int Ed*. 2020;59(23):9134-9142.
150. Shangguan X, Xu G, Cui Z, et al. Additive-assisted novel dual-salt electrolyte addresses wide temperature operation of lithium-metal batteries. *Small*. 2019;15(16):1900269.
151. Zhang X, Zou L, Xu Y, et al. Advanced electrolytes for fast-charging high-voltage lithium-ion batteries in wide-temperature range. *Adv Energy Mater*. 2020;10(22):2000368.
152. Andersson AM, Edström K. Chemical composition and morphology of the elevated temperature SEI on graphite. *J Electrochem Soc*. 2001;148(10):A1100-A1109.
153. Nagarajan S, Weiland C, Hwang S, Balasubramanian M, Arava LMR. Depth-dependent understanding of cathode electrolyte interphase (CEI) on the layered Li-ion cathodes operated at extreme high temperature. *Chem Mater*. 2022;34(10):4587-4601.
154. Yu Z, Zhang J, Wang C, et al. Flame-retardant concentrated electrolyte enabling a LiF-rich solid electrolyte interface to improve cycle performance of wide-temperature lithium-sulfur batteries. *J Energy Chem*. 2020;51:154-160.
155. Guo L, Huang F, Cai M, Zhang J, Ma G, Xu S. Organic-inorganic hybrid SEI induced by a new lithium salt for high-performance metallic lithium anodes. *ACS Appl Mater Interfaces*. 2021;13(28):32886-32893.
156. Zheng T, Xiong J, Zhu B, et al. From −20°C to 150°C: a lithium secondary battery with a wide temperature window obtainedviamanipulated competitive decomposition in electrolyte solution. *J Mater Chem A*. 2021;9(14):9307-9318.
157. Liao B, Li H, Xu M, et al. Designing low impedance interface films simultaneously on anode and cathode for high energy batteries. *Adv Energy Mater*. 2018;8(22):1800802.
158. Zhao D, Wang J, Lu H, Wang P, Liu H, Li S. Tailoring interfacial architecture of high-voltage cathode with lithium difluoro(bisoxalato) phosphate for high energy density battery. *J Power Sources*. 2020;456:228006.
159. Jones JP, Smart MC, Krause FC, Bugga RV. The effect of electrolyte additives upon lithium plating during low temperature charging of graphite-$LiNiCoAlO_2$ lithium-ion three electrode cells. *J Electrochem Soc*. 2020;167(2):020536.
160. Li Y, Cheng B, Jiao F, Wu K. The roles and working mechanism of salt-type additives on the performance of high-voltage lithium-ion batteries. *ACS Appl Mater Interfaces*. 2020;12(14):16298-16307.
161. Fan X, Wang C. High-voltage liquid electrolytes for Li batteries: progress and perspectives. *Chem Soc Rev*. 2021;50(18):10486-10566.
162. Liang G, Peterson VK, See KW, Guo Z, Pang WK. Developing high-voltage spinel $LiNi_{0.5}Mn_{1.5}O_4$ cathodes for high-energy-density lithium-ion batteries: current achievements and future prospects. *J Mater Chem A*. 2020;8(31):15373-15398.
163. Li M, Lu J, Chen Z, Amine K. 30 years of lithium-ion batteries. *Adv Mater*. 2018;30(33):1800561.
164. Xu K. Electrolytes and interphases in Li-ion batteries and beyond. *Chem Rev*. 2014;114(23):11503-11618.
165. Xue WJ, Gao R, Shi Z, et al. Stabilizing electrode-electrolyte interfaces to realize high-voltage Li||$LiCoO_2$ batteries by a sulfonamide-based electrolyte. *Energy Environ Sci*. 2021;14(11):6030-6040.
166. Xue W, Huang M, Li Y, et al. Ultra-high-voltage Ni-rich layered cathodes in practical Li metal batteries enabled by a sulfonamide-based electrolyte. *Nat Energy*. 2021;6(5):495-505.
167. Lu Z, Dahn JR. Can all the lithium be removed from T2-$Li_{2/3}[Ni_{1/3}Mn_{2/3}]O_2$? *J Electrochem Soc*. 2001;148(7):A710-A715.
168. Su CC, He M, Shi J, et al. Principle in developing novel fluorinated sulfone electrolyte for high voltage lithium-ion batteries. *Energy Environ Sci*. 2021;14(5):3029-3034.
169. Yoshida K, Nakamura M, Kazue Y, et al. Oxidative-stability enhancement and charge transport mechanism in glyme–lithium salt equimolar complexes. *J Am Chem Soc*. 2011;133(33):13121-13129.
170. Fox ET, Weaver JEF, Henderson WA. Tuning binary ionic liquid mixtures: linking alkyl chain length to phase behavior and ionic conductivity. *J Phys Chem C*. 2012;116(8):5270-5274.
171. Park J-W, Ueno K, Tachikawa N, Dokko K, Watanabe M. Ionic liquid electrolytes for lithium–sulfur batteries. *J Phys Chem C*. 2013;117(40):20531-20541.
172. Hu Z, Xian F, Guo Z, et al. Nonflammable nitrile deep eutectic electrolyte enables high-voltage lithium metal batteries. *Chem Mater*. 2020;32(8):3405-3413.

173. Zheng Q, Yamada Y, Shang R, et al. A cyclic phosphate-based battery electrolyte for high voltage and safe operation. *Nat Energy*. 2020;5(4):291-298.
174. Cao X, Ren X, Zou L, et al. Monolithic solid-electrolyte interphases formed in fluorinated orthoformate-based electrolytes minimize Li depletion and pulverization. *Nat Energy*. 2019;4(9):796-805.
175. Amanchukwu CV, Yu Z, Kong X, Qin J, Cui Y, Bao Z. A new class of ionically conducting fluorinated ether electrolytes with high electrochemical stability. *J Am Chem Soc*. 2020;142(16):7393-7403.
176. Ren X, Zou L, Cao X, et al. Enabling high-voltage lithium-metal batteries under practical conditions. *Joule*. 2019;3(7):1662-1676.
177. Suo L, Borodin O, Gao T, et al. "Water-in-salt" electrolyte enables high-voltage aqueous lithium-ion chemistries. *Science*. 2015;350(6263):938-943.
178. Liu K, Liu Y, Lin D, Pei A, Cui Y. Materials for lithium-ion battery safety. *Sci Adv*. 2018;4(6):eaas9820.
179. Rowden B, Garcia-Araez N. A review of gas evolution in lithium ion batteries. *Energy Rep*. 2020;6:10-18.
180. Rinkel BLD, Hall DS, Temprano I, Grey CP. Electrolyte oxidation pathways in lithium-ion batteries. *J Am Chem Soc*. 2020;142(35):15058-15074.
181. Camacho-Forero LE, Balbuena PB. Elucidating electrolyte decomposition under electron-rich environments at the lithium-metal anode. *Phys Chem Chem Phys*. 2017;19(45):30861-30873.
182. Chen X, Hou TZ, Li B, et al. Towards stable lithium-sulfur batteries: mechanistic insights into electrolyte decomposition on lithium metal anode. *Energy Storage Mater*. 2017;8:194-201.
183. Liu Y, Yu P, Wu Y, et al. The DFT-ReaxFF hybrid reactive dynamics method with application to the reductive decomposition reaction of the TFSI and DOL electrolyte at a lithium–metal anode surface. *J Phys Chem Lett*. 2021;12(4):1300-1306.
184. Markevich E, Sharabi R, Borgel V, et al. In situ FTIR study of the decomposition of N-butyl-N-methylpyrrolidinium bis (trifluoromethanesulfonyl) amide ionic liquid during cathodic polarization of lithium and graphite electrodes. *Electrochim Acta*. 2010;55(8):2687-2696.
185. Tian X, Yi Y, Fang B, et al. Design strategies of safe electrolytes for preventing thermal runaway in lithium ion batteries. *Chem Mater*. 2020;32(23):9821-9848.
186. Kong L, Li Y, Feng W. Strategies to solve lithium battery thermal runaway: from mechanism to modification. *Electrochemical Energy Rev*. 2021;4(4):633-679.
187. Shi P, Zheng H, Liang X, et al. A highly concentrated phosphate-based electrolyte for high-safety rechargeable lithium batteries. *Chem Commun*. 2018;54(35):4453-4456.
188. An K, Tran YHT, Kwak S, Han J, Song SW. Design of fire-resistant liquid electrolyte formulation for safe and long-cycled lithium-ion batteries. *Adv Funct Mater*. 2021;31(48):2106102.
189. Xu K, Zhang S, Allen JL, Jow TR. Nonflammable electrolytes for Li-ion batteries based on a fluorinated phosphate. *J Electrochem Soc*. 2002;149(8):A1079-A1082.
190. Jia H, Xu Y, Zhang X, et al. Advanced low-flammable electrolytes for stable operation of high-voltage lithium-ion batteries. *Angew Chem Int Ed*. 2021;60(23):12999-13006.
191. Feng X, Zhang Z, Li R, et al. New nonflammable tributyl phosphate based localized high concentration electrolytes for lithium metal batteries. *Sustain Energy Fuels*. 2022;6(9):2198-2206.
192. Liu S, Mao J, Zhang Q, et al. An intrinsically non-flammable electrolyte for high-performance potassium batteries. *Angew Chem Int Ed*. 2020;59(9):3638-3644.
193. Yang H, Guo C, Chen J, et al. An intrinsic flame-retardant organic electrolyte for safe lithium-sulfur batteries. *Angew Chem Int Ed*. 2019;58(3):791-795.
194. Liu S, Mao J, Zhang L, Pang WK, Du A, Guo Z. Manipulating the solvation structure of nonflammable electrolyte and interface to enable unprecedented stability of graphite anodes beyond 2 years for safe potassium-ion batteries. *Adv Mater*. 2021;33(1):2006313.
195. Liu X, Zheng X, Dai Y, et al. Fluoride-rich solid-electrolyte-interface enabling stable sodium metal batteries in high-safe electrolytes. *Adv Funct Mater*. 2021;31(30):2103522.
196. Zhang X, Lin X, Xu P, et al. Strong ion pairing at the origin of modified Li-cation solvation and improved performances of dual-salt electrolytes. *J Power Sources*. 2022;541:231644.
197. Xu N, Shi J, Liu G, et al. Research progress of fluorine-containing electrolyte additives for lithium ion batteries. *J Power Sources Adv*. 2021;7:100043.
198. Pham HQ, Lee HY, Hwang EH, Kwon YG, Song SW. Non-flammable organic liquid electrolyte for high-safety and high-energy density Li-ion batteries. *J Power Sources*. 2018;404:13-19.
199. Wang J, Lin F, Jia H, Yang J, Monroe CW, NuLi Y. Towards a safe lithium-sulfur battery with a flame-inhibiting electrolyte and a sulfur-based composite cathode. *Angew Chem Int Ed*. 2014;53(38):10099-10104.
200. Chen X, Yan S, Tan T, et al. Supramolecular "flame-retardant" electrolyte enables safe and stable cycling of lithium-ion batteries. *Energy Storage Mater*. 2022;45:182-190.
201. Le Bris K, DeZeeuw J, Godin PJ, Strong K. Radiative efficiency and global warming potential of the hydrofluoroether HFE-356mec3 ($CH_3OCF_2CHFCF_3$) from experimental and theoretical infrared absorption cross-sections. *J Mol Spect*. 2020;367:111241.

AUTHOR BIOGRAPHIES

Mingnan Li received his master's degree in 2021 from Hunan University, China. He is currently a PhD candidate at the University of Adelaide, under the supervision of Prof. Zaiping Guo. His research is focused on the design of electrolytes for Li metal batteries as well as electrolyte/electrode interface optimization.

Caoyu Wang received his BS and Master degrees from Huazhong Agricultural University. He is currently a PhD candidate under the supervision of Prof. Zaiping Guo at the School of Chemical Engineering and Advanced Materials,

The University of Adelaide, Australia. His current research interests focus on the design and application of alkali-metal anodes for rechargeable batteries.

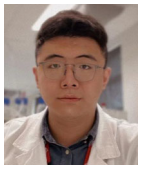

Jingxi Li is currently a PhD student at the University of Adelaide, under Professor Zaiping Guo's supervision. He received his master's degree at the University of Wollongong in 2022. His research is focusing on the development of Ni-rich layered cathode materials for high-energy lithium-ion batteries.

Guanjie Li received his master's degree from the South China Normal University in 2020. He is currently a PhD candidate at University of Adelaide, under the supervision of Prof. Zaiping Guo. His current research interests focus on the design of functional electrolytes for zinc-ion batteries, and the properties of electrode/electrolyte interface.

Dr Shilin Zhang is now a research fellow in the University of Adelaide, Adelaide, Australia. He received his PhD degree from the Institute of Superconducting & Electronic Materials at the University of Wollongong (Australia) in 2020, under the supervision of Prof. Zaiping Guo. His current research interests focus on the design, synthesis and characterization of materials in the field of electrochemical devices such as ion batteries and metal batteries.

Dr. Jianfeng Mao received his PhD degree in materials engineering from the University of Wollongong, Australia. He has been working at the Max-Planck-Institute fürKohlenforschung, University of Glasgow, University of Maryland, University of Wollongong, and the University of Adelaide. His current research interests focus on the development of advanced electrode and electrolyte materials for batteries as well as battery recycling.

Professor Zaiping Guo is an ARC Australian Laureate Fellow at the School of Chemical Engineering & Advanced Materials, The University of Adelaide. She received her PhD degree in Materials Engineering from the University of Wollongong in 2003. Before joining the University of Adelaide, she was a Distinguished Professor at the University of Wollongong. Her research focuses on the design and application of electrode and electrolyte materials for energy storage and conversion, including rechargeable batteries, hydrogen storage, and fuel cells.

How to cite this article: Li M, Wang C, Davey K, et al. Recent progress in electrolyte design for advanced lithium metal batteries. *SmartMat*. 2023;4:e1185. doi:10.1002/smm2.1185